ESL-TR-90-16

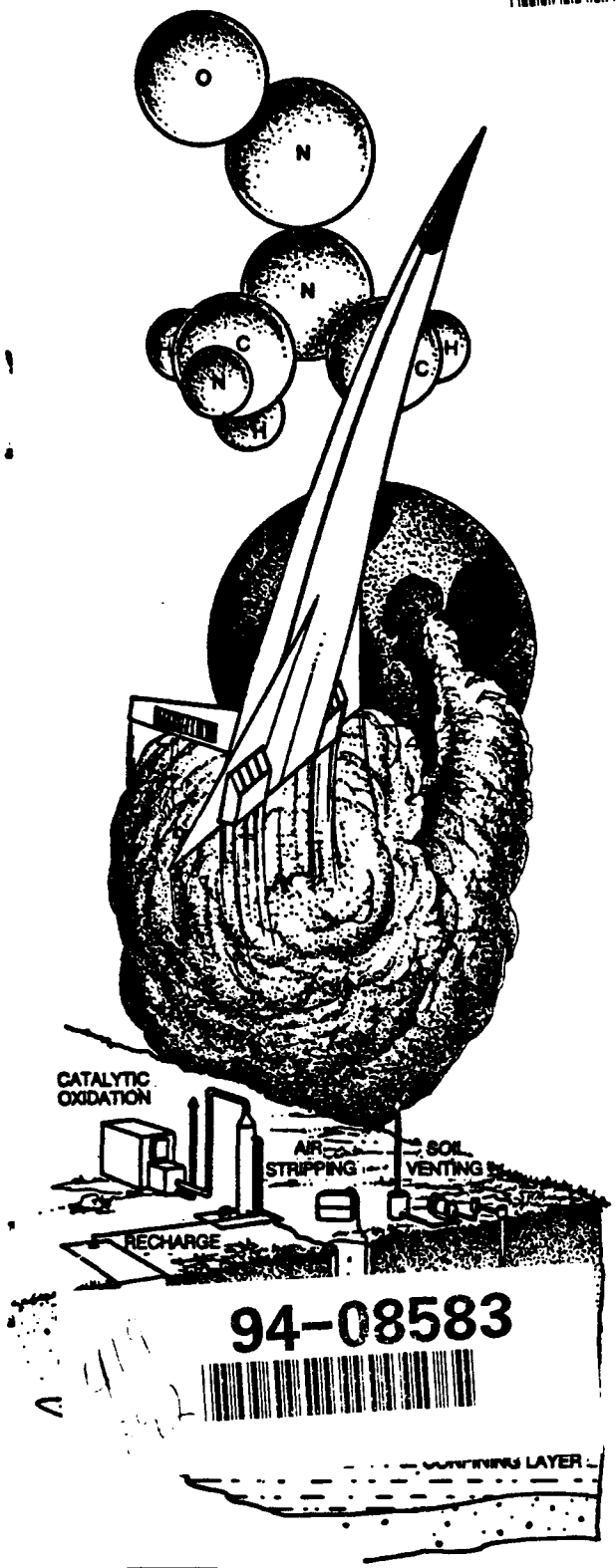

PHOTOTHERMAL LASER DEFLECTION, AN INNOVATIVE TECHNIQUE TO MEASURE PARTICLES IN EXHAUSTS

DR. CECIL F. HESS

METROLASER
18006 SKYPARK CIRCLE, #108
IRVINE CA 92714-6428

OCTOBER 1993

FINAL REPORT

AUGUST 1989 - FEBRUARY 1990

ENVIRONICS DIVISION
Air Force Engineering & Services Center
ENGINEERING & SERVICES LABORATORY
Tyndall Air Force Base, Florida 32403

NOTICE

PLEASE DO NOT REQUEST COPIES OF THIS REPORT FROM HQ AFESC/RD (ENGINEERING AND SERVICES LABORATORY). ADDITIONAL COPIES MAY BE PURCHASED FROM:

NATIONAL TECHNICAL INFORMATION SERVICE
5285 PORT ROYAL ROAD
SPRINGFIELD, VIRGINIA 22161

FEDERAL GOVERNMENT AGENCIES AND THEIR CONTRACTORS REGISTERED WITH DEFENSE TECHNICAL INFORMATION CENTER SHOULD DIRECT REQUESTS FOR COPIES OF THIS REPORT TO:

DEFENSE TECHNICAL INFORMATION CENTER
CAMERON STATION
ALEXANDRIA, VIRGINIA 22314

Report Documentation Page

UNCLASSIFIED
SECURITY CLASSIFICATION OF THIS PAGE

REPORT DOCUMENTATION PAGE

Form Approved OMB No 0704-0188

1a REPORT SECURITY CLASSIFICATION: UNCLASSIFIED	1b RESTRICTIVE MARKINGS
2a SECURITY CLASSIFICATION AUTHORITY	3 DISTRIBUTION/AVAILABILITY OF REPORT: Approved for Public Release Distribution Unlimited
2b DECLASSIFICATION/DOWNGRADING SCHEDULE	
4 PERFORMING ORGANIZATION REPORT NUMBER(S)	5 MONITORING ORGANIZATION REPORT NUMBER(S): ESL-TR-90-16
6a NAME OF PERFORMING ORGANIZATION: MetroLaser; 6b OFFICE SYMBOL (If applicable): 0 DLL8	7a NAME OF MONITORING ORGANIZATION: Air Force Engineering and Services Center
6c ADDRESS (City, State, and ZIP Code): 18006 Skypark Circle, #108 Irvine, CA 92714-6428	7b ADDRESS (City, State, and ZIP Code): HQ AFESC/RDVS Tyndall AFB FL 32403-6001
8a NAME OF FUNDING/SPONSORING ORGANIZATION: HQ AFESC/RDVS; 8b OFFICE SYMBOL (If applicable): FQ7621	9 PROCUREMENT INSTRUMENT IDENTIFICATION NUMBER: F08635-89-C-0350
8c ADDRESS (City, State, and ZIP Code): Tyndall AFB, FL 32403-6001	10 SOURCE OF FUNDING NUMBERS: PROGRAM ELEMENT NO. 65502F; PROJECT NO. 3005; TASK NO. 00; WORK UNIT ACCESSION NO 51

11 TITLE (Include Security Classification): Photothermal Laser Deflection, an Innovative Technique to Measure Particles in Exhausts

12 PERSONAL AUTHOR(S): Dr. Cecil F. Hess

13a TYPE OF REPORT	13b TIME COVERED	14 DATE OF REPORT (Year, Month, Day)	15 PAGE COUNT
Final	FROM 89/8/2 TO 90/2/	October 1993	37

16 SUPPLEMENTARY NOTATION: Prepared in cooperation with Vanderbilt University

17 COSATI CODES			18 SUBJECT TERMS (Continue on reverse if necessary and identify by block number)
FIELD	GROUP	SUB GROUP	smoke and gaseous concentration, laser diagnostics, photothermal deflection
04	01		
07	04		

19 ABSTRACT (Continue on reverse if necessary and identify by block number)

Purpose of work

The purpose of this Phase I work was to demonstrate the feasibility of using an optical technique called Photothermal Laser Deflection (PLD) to measure the concentration of airborne soot from 0.1 to 10 mg/m^3, and NO_2 from 2 to 200 ppm. These concentration ranges are of interest to the gas turbine and rocket communities. PLD employes a laser to heat a small volume of gas containing the absorbing species of interest, thereby creating a refractive index gradient in the gas. A second laser beam crosses this heated region and is temporarily deflected by the refractive index gradient. The amount of deflection is proportional to the mass loading of the absorbing species. *(continued on back)*

20 DISTRIBUTION/AVAILABILITY OF ABSTRACT	21 ABSTRACT SECURITY CLASSIFICATION
☒ UNCLASSIFIED/UNLIMITED ☐ SAME AS RPT. ☐ DTIC USERS	UNCLASSIFIED
22a NAME OF RESPONSIBLE INDIVIDUAL: Captain Mark Smith	22b TELEPHONE (Include Area Code): 904-283-4234; 22c OFFICE SYMBOL: RDVS/34234

DD Form 1473, JUN 86 — Previous editions are obsolete. — SECURITY CLASSIFICATION OF THIS PAGE

UNCLASSIFIED

Description of work
A breadboard PLD system was designed and built to measure the concentration of both soot and NO_2. The system employed a pulsed excimer-pumped dye laser operating at 451 nm as the pump source, and a Helium-Neon laser as the probe. Probe beam deflection was detected with a bi-cell detector, and measured with a lock-in amplifier. A soot generator was developed to produce submicron soot at concentrations spanning the range from 0.1 to 10 mg/m^3. An analytical model was developed and a sensitivity analysis was performed relating probe beam deflection to NO_2 concentration. A series of experiments were conducted to measure the concentration of both soot and NO_2 under controlled laboratory conditions. Recommendations for further work and for improving the sensitivity of a second generation system were explored in detail.

Findings
The experiments and analyses conducted during Phase I demonstrated the feasibility of PLD in measuring the mass concentration of both soot particles and NO_2 at a repetition rate of 25 Hz. PLD response was linear at soot concentrations from 0.3 to 10 mg/m^3, and at NO_2 concentrations from approximately 6 to 200 ppm. Strategies to measure lower concentrations have been defined and include focusing the probe beam onto the face of the bi-cell detector. The large dynamic range, fast acquisition rate, and ability to measure both particulate and gaseous pollutants makes PLD superior to other available methods.

Applications
PLD will find applications in measuring exhaust particles and gaseous pollutants such as NO_x from military and commercial internal combustion, diesel, and gas turbine engines, and rockets. With additional work, PLD may be successful in measuring other polluting gases and particles (e.g., Freon and asbestos). Its fast time response makes PLD an excellent candidate for *in situ* measurements under many conditions, including turbulent and combusting flows.

SUMMARY

Photothermal Laser Deflection (PLD) is an analytical technique to measure in real-time the mass concentration of particles and gaseous exhaust pollutants in a variety of combustion devices (e.g., gas turbine engines and rockets). PLD uses a pump laser to locally heat the particle or gaseous species, thus changing the refractive index of the surrounding gas to form a thermal lens. A probe laser beam traveling through the thermal lens is temporarily deflected, and the amount of deflection is proportional to the species mass concentration.

The experiments and analyses conducted during Phase I demonstrated the feasibility of PLD in measuring the mass concentration of both soot particles and NO_2 at a repetition rate of 25 Hz. PLD response was linear at soot concentrations from 0.3 to 10 mg/m^3, and at NO_2 concentrations from approximately 6 to 208 ppm. Strategies to measure lower concentrations have been defined and include focusing the probe beam onto the face of the bi-cell detector. The large dynamic range, fast acquisition rate, and ability to measure both particulate and gaseous pollutants makes PLD superior to other available methods.

PLD measurements were made with a breadboard system employing a pulsed excimer-pumped dye laser operating at 451 nm as the pump source, and a Helium-Neon laser as the probe. Probe beam deflection was detected with a bi-cell detector, and measured with a lock-in amplifier. A soot generator was developed to produce submicron soot at concentrations spanning the range from 0.1 to 10 mg/m^3. An analytical model was developed and a sensitivity analysis was performed relating probe beam deflection to NO_2 concentration. A series of experiments were conducted to measure the concentration of both soot and NO_2 under controlled laboratory conditions. Recommendations for further work and for improving the sensitivity of a second generation system were explored in detail.

The PLD technique will find application in measuring exhaust particles from internal combustion and diesel engines, gas turbine engines, and rockets. It can also measure NO_2, and has the potential to measure other solid and gaseous species such as asbestos, chlorofluorocarbons (i.e., freons), and various products of combustion. The technique can be a powerful diagnostic tool in both research, industry, and government, with applications in combustion, air quality monitoring and enforcement, and environmental and pollution studies.

(The reverse of this page is blank)

PREFACE

This report was prepared by MetroLaser, 18006 Skypark Circle, Suite 108, Irvine, California, under Contract Number F08635-89-C-0350, for the Air Force Engineering and Services Center, Engineering and Services Laboratory (AFESC/RDVS), Tyndall Air Force Base, Florida 32403-6001. Capt Mark D. Smith, was the Government technical program manager. The report summarizes work accomplished between 2 August 1989 and 2 February 1990.

MetroLaser would like to extend special thanks to Professor Robert Pitz at Vanderbilt Unviersity for his valuable assistance in the analytical and experimental efforts reported here, and to Mr Tom Brown, also at Vanderbilt University, for his assistance in the construction and conduct of the experiments performed in Phase I.

This report has been reviewed by the Public Affairs Office and is releasable to the National Technical Information Service (NTIS). AT NTIS, it will be available to the general public, including foreign nations

This technical report has been reviewed and is approved for publication.

MARK D. SMITH, Capt, USAF, BSC
Project Officer

NEIL J. LAMB, Colonel, USAF, BSC
Chief, Environics Division

WAYNE P. CHEPREN, Maj, USAF
Chief, Pollution Prevention and
Environmental Compliance Branch

FRANK P. GALLAGHER III, Colonel, USAF
Director, Air Force Civil Engineering
Laboratory

(The reverse of this page is blank.)

TABLE OF CONTENTS

LIST OF FIGURES

LIST OF ABBREVIATIONS

Å	angstrom
C	degrees Centigrade
cc	cubic centimeters
cm	centimeter
g	gram
Hz	hertz
J	joules
K	degrees Kelvin
Kg	Kilogram
kHz	kilohertz
m	meter
mg	milligram
mJ	millijoules
ml	milliliters
mm	millimeter
ms	milliseconds
mV	millivolts
nm	nanometer
ns	nanoseconds
ppm	parts per million

LIST OF SYMBOLS

a	$1/e^2$ radius of pump beam (meters)
A_A	mass specific absorption coefficient of absorbing species (meter^2/gram)
c_p	specific heat of medium (joules/kilogram-kelvin)
d	probe beam diameter at bi-cell detector (meters)
D	diffusivity of medium (meter^2/second)
E_O	energy per laser pulse (joules)
K	proportionality constant relating ϕ_{max} to ρ
l	interaction length between probe and pump beams (meters)
m_a	mass of dry air per unit volume (grams/cubic centimeter)
m_v	mass of water vapor per unit volume (grams/cubic centimeter)
$\frac{\partial n}{\partial T}$	change in refractive index with temperature at constant pressure
n_0	unperturbed refractive index
P	probe beam power at detector face (watts)
R	distance from sample cell output window to bi-cell detector (meters)
S	radiant sensitivity at photodetector
t	time
t_o	duration of laser pulse
V_{max}	measured voltage from detector for a probe beam deflection of ϕ_{max}
v_x	velocity in x-direction (meter/second)
w	humidity ratio
x	separation between probe and pump beams (meters)
x_{max}	separation between probe and pump beams (meters) which results in the maximum probe beam deflection ϕ_{max}

LIST OF SYMBOLS
(CONCLUDED)

α	absorption coefficient of absorbing species (meter^{-1})
Θ	divergence of probe beam (radians)
ρ	mass loading of absorbing species (kilogram/meter^3)
ρ_m	density of medium (kilogram/meter^3)
ϕ_{max}	maximum probe beam deflection (radians)
$\phi_j(x,y,t)$	probe beam deflection (radians) as a function of spatial coordinates, x and y, and time, t
Ω	input impedence of signal measuring equipment (ohms)

SECTION I

INTRODUCTION

A. OBJECTIVES

Two major objectives were pursued during Phase I:

1. Evaluate the feasibility of PLD to measure, in real time, the mass concentration of soot particles and nitrogen dioxide (NO_2) representative of jet engines and rockets. In consultation with the program manager at Tyndall Air Force Base, the appropriate range of concentrations was defined as 0.1 to 10 mg/m^3 for soot, and 2 to 200 ppm for NO_2.

2. Define possible configurations that can lead to a field product.

To help meet the above objectives, two additional objectives were pursued:

1. Establish the theoretical basis of the PLD technique in the measurement of exhaust particles. This included the development of the relationship between probe beam deflection and gas or particle mass loading for the specific experimental geometry used in this study, and an analysis of technique sensitivity based on these relationships.

2. Experimentally verify the performance of PLD under controlled laboratory conditions. This included the design and construction of an experimental breadboard incorporating a pulsed pump laser, and the development of a soot particle generator to simulate the size distribution and mass loading of realistic exhaust environments.

The theoretical studies and the development of the soot particle generator were conducted by MetroLaser in Irvine, California. The experimental effort was performed at the Combustion Laboratory at Vanderbilt University in Nashville, Tennessee, by technical personnel from both MetroLaser and the University.

B. BACKGROUND

Particle measurement devices with increased sensitivities and faster response times are needed to measure the mass concentration of particles in the exhaust of jet engines and rockets. These particles have environmental, tactical, and performance effects important to the Air Force, the Environmental Protection Agency, other government agencies, and to the aerospace and automobile industries. These effects are particularly important in light of the new generation of high-performance fuels which will soon be in use, and with the tougher air quality control policies. Examples of particles of interest are rocket exhaust particles, diesel and gas turbine engine soot, asbestos, and naturally occurring atmospheric particles.

In addition to measuring particles, the Air Force and other government and state agencies are interested in measuring gaseous exhaust pollutants such as NO_x. Thus, the ideal instrument will simultaneously measure a spectrum of pollutants and provide real-time assessment of pollutant concentrations.

Photothermal laser deflection (PLD) has been shown to provide this information accurately and with extremely fast time response. Phase I experiments successfully measured the mass concentration of soot particles in concentrations from 0.3 to 10 mg/m^3,

and NO_2 concentrations from 6 to 208 ppm, at rates of 25 times per second. Numerical analysis showed that these ranges can be extended down by at least a factor of 4 and up by a factor of 10. In contrast, current smoke meters use filtering techniques which provide time-averaged information with collection times as long as 20 minutes, and many currently available instruments lack the sensitivity of PLD. Thus, PLDs combined capability of measuring particles, as well as gaseous pollutants over a broad range of concentrations and in a fraction of a second, gives it unique and needed capabilities.

PLD is a spectroscopic technique first explored extensively in the early 1980s as a viable candidate for measuring various properties of gases having absorption lines that can be probed with commercially available lasers (e.g., References 1-3). Since then, researchers have explored various applications of PLD, including the measurement of temperature, flow velocity, species concentration, and selected physical properties (e.g., References 4-7), and have demonstrated the usefulness of this technique for combustion diagnostics, including the measurement of soot concentration (e.g., References 8-12). In fact, in a recent survey (Reference 13), the PLD technique was recommended as one of the most promising techniques for measuring smoke from engine exhaust.

The PLD technique has been recently reported to satisfy, in principle, the following criteria for an ideal diagnostic technique, giving it advantages over many other analytical techniques (Reference 14):

1. Measurements can be made in situ.

2. Measurements are essentially nonperturbing. Only very small temperature changes are induced by the pump beam.

3. It has a high sensitivity. It is therefore suitable for measuring minority species, and very small soot concentrations.

4. A high degree of spatial resolution can be achieved by crossing the probe and pump beams at or near right angles.

5. High temporal resolution is achieved using a pulsed light source.

6. Absolute measurements of concentration are possible because the technique is virtually insensitive to the rate of quenching collisions.

7. More than one species can be measured in rapid succession by pumping the sample volume sequentially with more than one laser wavelength.

Various PLD review articles have been published (References 15-17) and the increasing interest in the PLD technique has resulted in the publication of an excellent book on the subject (Reference 14).

Figure 1 illustrates the basic principle of the PLD technique. Following the discussions in References 14 and 17, a laser beam, called the pump beam, passes through and heats up the region of interest. The PLD technique requires a modulation in the pump beam which can be in the form of short intense pulses (typically 20 to 50 ns in duration, containing 5 to 20 mJ of energy, produced at 10 to 100 pulses per second), or a continuous train of pulses at nearly 50 percent duty cycle (this pump beam could come from a diode laser, an arc lamp, or a tunable dye laser, depending on the application). The laser wavelength is chosen to coincide with an absorption line or band of the species to be detected, and the species then absorbs energy from the pump beam. (When measuring

soot, the choice of irradiation wavelength is often less critical because soot absorbs energy throughout the ultraviolet, visible, and infrared). If the species is a gas and the pressure is sufficiently high (i.e., if the quenching collisional rates are sufficiently fast compared to the radiative rates), most of the energy quickly appears in the rotational-translational modes of the medium. Thus, for most gaseous species at atmospheric pressure only a negligible fraction of the energy is emitted as fluorescence, and the irradiated region becomes slightly heated. If two phases are involved (e.g., soot in air or nitrogen), the heat transfer process is more complicated because heat must be transferred from the solid to the gas phase, but the result is the same: the irradiated region becomes slightly heated.

The heating of the irradiated region results in changes in the refractive index of the medium in that region. If the density of the absorbing species is uniform over the width of the pump beam, the refractive index acquires a spatial profile which is a mirror image of the intensity distribution of the pump beam (generally assumed to be Gaussian). The resulting refractive index gradient is caused by the decreased density of the medium due to the local temperature rise, and decays in time following the diffusional decay of the temperature profile.

The PLD technique uses a second laser beam, called the probe beam, whose centerline is displaced slightly from that of the pump beam. The angle of overlap between the probe beam and the pump beam can be chosen from near parallel (to maximize the interaction length, and hence the sensitivity) to perpendicular (to maximize the spatial resolution). The probe beam, which in Phase I was the 633 nm line of a He-Ne laser, is deflected due to variations in the refractive index of the medium created by the pump beam. This deflection can be easily measured by a position-sensitive optical detector, and is proportional to the number density (i.e., the concentration) of the absorbing molecules. Therefore, the PLD technique can be used to measure majority and minority species concentrations. If a pulsed pump laser is used to measure a gaseous species, the probe beam is deflected almost instantaneously, following the laser firing, and gradually returns to its original position on the time scale of the diffusion time of the heat from the irradiated region. If a pulsed pump laser is used to measure a solid species such as soot, the probe beam deflects more slowly because of the additional step in transferring heat from the soot to the surrounding gas. However, the results of Phase I show that the time scale associated with heating soot particles was only slightly slower than for heating NO_2. The theoretical aspects of PLD pertinent to this program are discussed in Section II.

C. SCOPE

The work conducted under Phase I was organized under the following nine tasks:

Task 1. An optimal pump laser wavelength was chosen.

Task 2. A theoretical model was developed relating the probe beam deflection to the mass loading of the gaseous species being measured.

Task 3. A sensitivity analysis was performed relating probe beam deflection to mass concentration.

Task 4. An experimental configuration was designed and built.

Task 5. An experimental parametric matrix was developed.

Task 6. Experiments were conducted at Vanderbilt University.

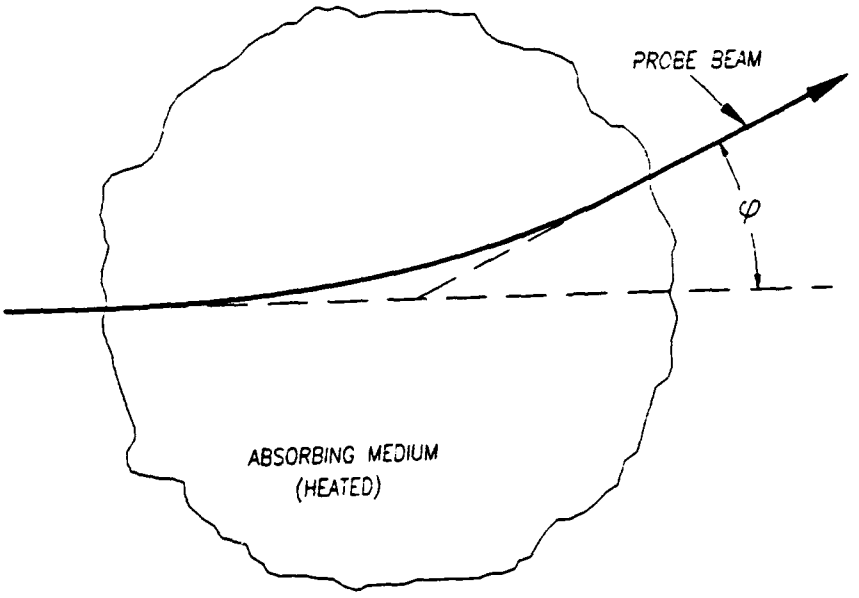

Figure 1. Schematic of the Deflection of the Probe Beam as it Passes through a Heated Medium.

Task 7. Experimental data were analyzed and reconciled with the theoretical predictions.

Task 8. Prototype configurations leading to a field product were defined.

Task 9. Periodic progress reports were written and the final report was prepared.

SECTION II

THEORETICAL DISCUSSION OF PHOTOTHERMAL LASER DEFLECTION

The amplitude of the PLD signal depends on the concentration of the absorbing species and on the temperature and flow velocity to minimize complexity. Phase I measurements were thus made under isothermal, no-flow conditions. This section will discuss the analytical expressions governing the PLD signals generated under the experimental conditions used in Phase I.

A. PRELIMINARY DESCRIPTION OF PROBE AND PUMP LASER BEAM GEOMETRY

The preliminary description of the specific probe and pump beam geometry used in Phase I provides a physical basis for the theoretical discussions presented in this section. A more extensive description of the experimental facility is given in Section III.

Figure 2 shows the orientation of the probe and pump beams relative to the coordinate system adopted for use in Phase I. This coordinate system is the same as that used by Rose, Gupta, and co-workers for their mathematical derivations (References 14 and 17) in which the pump beam is assumed to be coaxial with both the centerline of the sample cell (described in Section III) and the z-axis. The probe beam was placed slightly above the pump beam (in the x-direction) and was angled 0.75 degrees in the y-z plane with respect to the pump beam to avoid the superposition of the two beams on the sample windows. Thus, the case studied here was essentially **collinear PLD**, as opposed to transverse PLD (where the beams cross at right angles). Using the collinear case in Phase I maximized the interaction volume of the two beams, which maximized sensitivity at the expense of unneeded spatial resolution.

B. PROBE BEAM DEFLECTION WITH A PULSED PUMP LASER IN A GASEOUS MEDIUM

Measurements taken during Phase I were obtained with a pulsed excimer-pumped dye laser (described in Section III) with a pulse duration of approximately 30 ns. (The choice of this laser was circumstantial and, in general, much simpler lasers or other light sources could be used). Because of the short duration of the laser pulse used in Phase I, the theoretical relationships governing probe beam deflection can be simplified significantly using an approximation referred to as the impulse approximation, which requires that the pulse duration be less than 1 microsecond. Rose, et al. (Reference 17) have derived the following time-dependent analytical expression describing the deflection of the probe beam in radians, $\phi_1(x,y,t)$, in a **gaseous medium** for the collinear case using the impulse approximation:

$$\phi_1(x,y,t) = -\frac{\partial n}{\partial T}\,\frac{8l\,\alpha E_o(x-v_x t)}{n_0 \pi \rho_m c_p (8Dt+a^2)^2}\,\exp\left[\frac{-2((x-v_x t)^2+y^2)}{8Dt+a^2}\right] \qquad (1)$$

where l = interaction length (meters)
n_0 = unperturbed refractive index
$\partial n/\partial T$ = change in refractive index with temperature (K^{-1}) at constant pressure

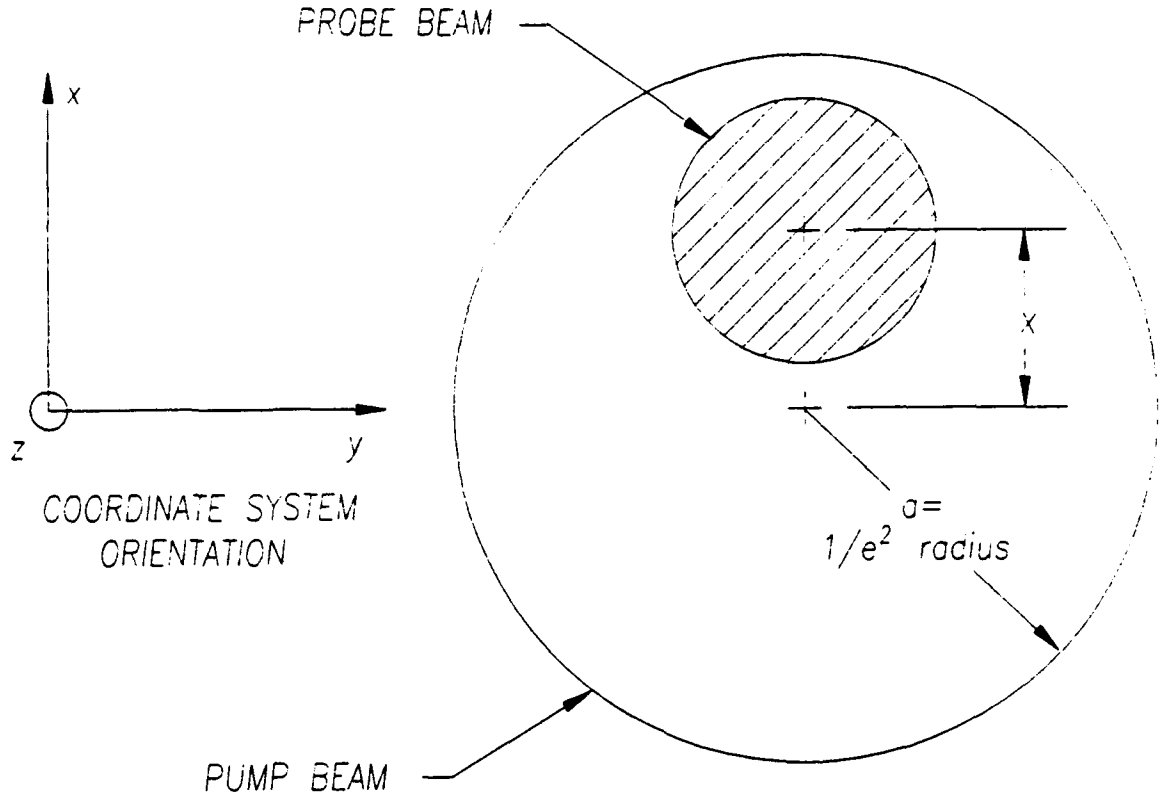

Figure 2. **Orientation of Probe and Pump Beams Relative to the Coordinate System Used in Phase I.**

α = absorption coefficient of absorbing species (meters^{-1})
E_o = energy per laser pulse (joules)
ρ_m = density of medium (kg/meter^3)
c_p = specific heat of medium (joules/kg-K)
v = velocity in x-direction (meters/second)
D = diffusivity of medium (meters^2/second)
a = $1/e^2$ radius of pump beam (meters)

Note that the parameter x is the separation between the probe and pump beams (in meters). Note also that the equation relating beam deflection to soot concentration will be different than Equation (1) (which was derived for a gaseous species) because of the added heat transfer mechanism between the particles and the surrounding gas. However, Equation (1) was used in this study to approximately describe the probe beam deflection when measuring soot.

The parameter α in Equation (1) is proportional to the mass loading, ρ, of the absorbing species:

$$\alpha = \rho A_A$$

where ρ = mass loading of absorbing species (kg/m^3)
A_A = mass specific absorption coefficient of absorbing species (m^2/g)

The absorption coefficient of soot is also characterized by a similar parameter α for low particle concentrations where scattering is negligible, which is a very good approximation for the work reported here. The parameter A_A is not a function of soot diameter in the Rayleigh regime (i.e., diameters less than 0.1 micrometer) and is essentially constant at the constant irradiation wavelength used in Phase I. Values for A_A used in Phase I for soot and NO_2 are 10 m^2/g and 0.34 m^2/g, respectively (Reference 13).

In addition to the stipulation that the pulse width be less than 1 microsecond, Equation (1) was derived assuming the following:

- Inhomogeneities in the medium along the pump beam are negligible. This implies the problem is two-dimensional in that the effect of thermal diffusion along the z-direction is negligible.
- The medium is weakly absorbing.
- The pump beam has a Gaussian intensity profile.
- The laser has a rectangular temporal profile (meaning the laser pulse turns on sharply at time t = 0, and turns off sharply at t = t_o).
- The effect of the pressure pulse (the photoacoustic effect) accompanying the photothermal signal in negligible.
- The probe beam is infinitesimally thin.

Equation (1) can now be used to determine the specific value of the separation between the probe and pump beams, called x_{max}, which results in the maximum probe beam

deflection, ϕ_{max}. This is accomplished by first differentiating Equation (1) with respect to x, then setting the resulting equation equal to zero. Solving for x gives:

$$x = (a^2/4 + 2Dt)^{\frac{1}{2}} + v_x t \tag{2}$$

Thus, as time increases after the initial pump laser pulse, the distance between the pump beam centerline and the location giving maximum deflection increases. This casts the problem in a different light: we now wish to find both the time (relative to the pump beam firing) and the location (relative to the pump beam centerline) which gives ϕ_{max}. If Equation (2) is substituted back into Equation (1), it becomes clear that the maximum probe beam deflection, ϕ_{max}, occurs at t = 0. (This is not expected to be true for soot particles since the heat transfer from the particles to the surrounding gas takes place over a finite time.) Substituting t = 0 into Equation (2) shows that ϕ_{max} occurs when the beam separation is $x_{max} = a/2$. In summary, for gases:

$$\phi_{max} \text{ occurs when: } t = 0 \text{ and } x_{max} = a/2.$$

Equation (1) can now be modified to apply to the specific experimental configuration used in Phase I. Substituting t = 0, x = a/2, and y = 0 (in Phase I, the probe beam had no y-displacement relative to the pump beam) into Equation (1) results in the following relationship for ϕ_{max} (in radians) pertinent to making gas phase (e.g., NO_2) measurements in Phase I:

$$\phi_{max} = -\frac{\partial n}{\partial T} \frac{4l\ \alpha E_o}{n_0 \pi \rho_m c_p a^3} \exp\ [-0.5] \tag{3}$$

This equation can be simplified to :

$$\phi_{max} = K\rho \tag{4}$$

where K is a constant and, as discussed above, $\rho = \alpha/A_A$ = the mass loading of absorbing species in kg/m^3. The experiments performed in Phase I show that this linear behavior is also true for soot particles.

C. PROBE BEAM DEFLECTION IN A TWO-PHASE FLOW

A major objective of Phase I was the demonstration of the feasibility of measuring the mass concentration of soot particles using PLD. The experimental results discussed later in this report demonstrate that the PLD signal is linearly dependent on the soot mass concentration. For the purposes of Phase I, the relationship between probe beam deflection and the mass loading of the solid particulate in a two-phase flow was assumed to be given by Equation (4). A more complete derivation will be conducted in Phase II to account for the additional complexity inherent in transferring heat from the soot to the surrounding gas in the establishment of the necessary refractive index gradient. A brief description of the complexity of this two-phase process is presented here, as an introduction.

There are two regimes involving the absorption of energy by soot particles; 1) the pump energy is large and the particles are vaporized, and 2) the pump energy is low and the particles are heated. The time scales of the heat transfer to the gaseous medium associated with these two regimes are expected to be very different. Since the ultimate goal is to demonstrate the PLD technique *in situ* in environments of interest to the Air Force, understanding and quantifying the heat transfer time scales is essential. Phase I results show that extremely fast measurements were possible with soot particles suggesting that they are vaporized by the pump beam.

Whereas maximum probe beam deflection occurs at t = 0 when measuring gaseous species (because of the fast rate of collisional energy transfer), the additional heat transfer step and the specific distribution of mass described above will result in a delay in attaining maximum deflection in a two-phase flow. The magnitude and timing of the deflection will be modeled with the relationship to be derived in Phase II.

D. SENSITIVITY ANALYSIS FOR NO_2 USING FAR-FIELD APPROXIMATION

In this section, the relationship between maximum beam deflection angle, ϕ_{max} (in radians), and the measured signal voltage using the far-field approximation is derived. This approximation assumes that the distance between the probe laser and the bi-cell detector is large enough that the probe beam is diverging at a constant angle (equal to the published divergence angle of the specific laser used). A sensitivity analysis of the PLD technique is then performed for the measurement of NO_2 using typical Phase I values.

In general, however, the far-field solution derived here is not applicable since the distance between the probe laser and the bi-cell detector should be kept to a minimum in order to minimize vibration and thermal effects. Under this condition (i.e., the **near-field** case), it is appropriate to assume that the probe beam diameter remains constant and equal to the laser waist diameter. The near-field solution and its effect on the calculated PLD sensitivity will be developed in detail in Phase II, and will be extended to include the measurement of soot.

Figure 3 shows a schematic representation of the deflected probe beam. For analysis, ϕ_{max} is the maximum deflection which occurs at t = 0 when the probe and pump beams are separated a distance of x = a/2, calculated using Equation (3). R is the distance (in meters) from the output window of the sample cell to the bi-cell.

Figure 4 shows a schematic of the deflected probe beam on the face of the bi-cell photodetector. The shaded portion is the area of the beam which has moved from the lower half of the bi-cell to the upper half as a result of photothermal deflection. This distance, $R\ \phi_{max}$ (in meters), is usually small relative to the beam diameter, d (in meters), on the face of the photodetector, and the shaded area can be approximated by a rectangle of area $R\ \phi_{max} d$. The shaded area relative to the area of the beam on the face of the photodetector is:

$$\text{relative area} = R\,\phi_{max} d/(\pi d^2/4) = 4R\,\phi_{max}/\pi d.$$

Furthermore, in the far field, the beam diameter, d, can be expressed as $R\ \theta$, where θ is the divergence of the probe beam (in radians). Therefore, the relative shaded area in Figure 4 is:

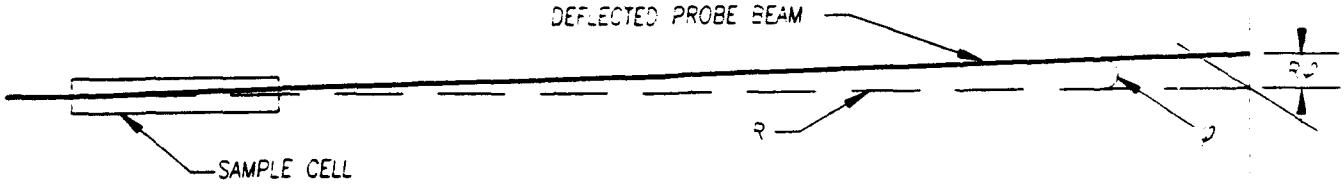

Figure 3. Schematic of Deflected Probe Beam

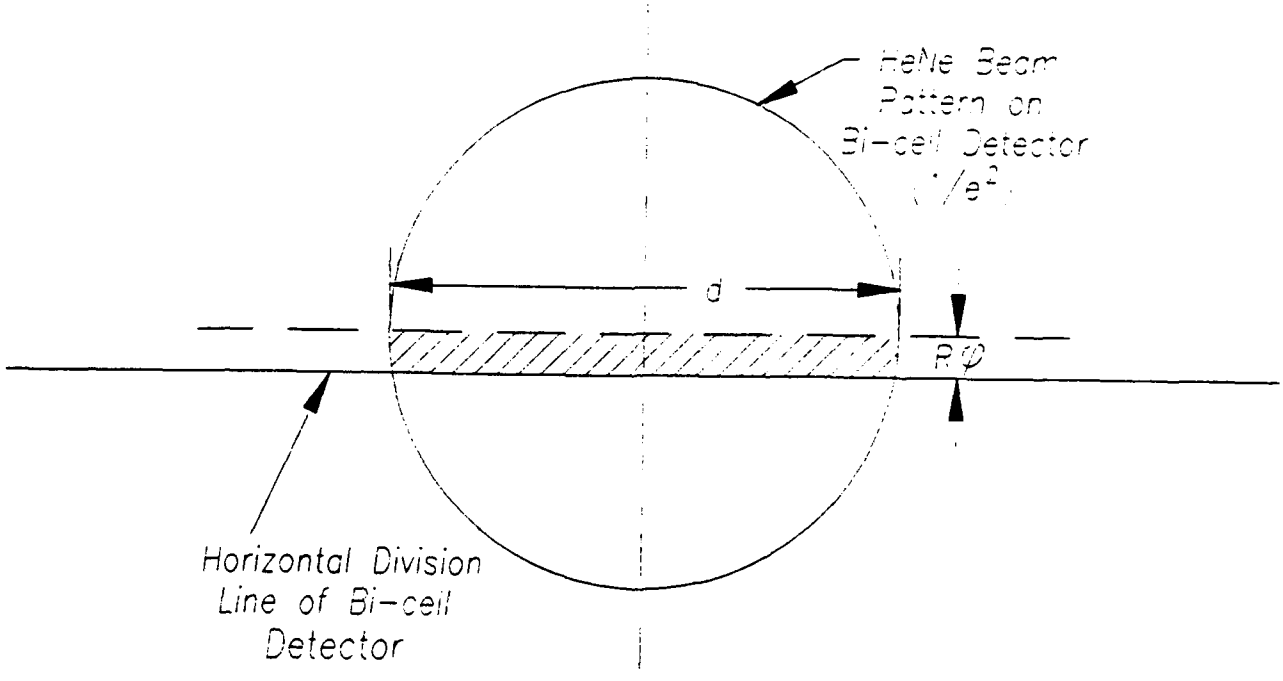

Figure 4. Schematic of Deflected Probe Beam on the Face of the Bi-Cell Detector.

$$\text{relative area} = 4R\phi_{max}/\pi R\theta = 4\phi_{max}/\pi\theta = 1.273\,(\phi_{max}/\theta).$$

The radiant power in the shaded area of Figure 4 is equal to the probe beam power at the detector face, P (in watts), times the relative area of the shaded portion:

$$\text{power in shaded area} = 1.273\,P\,(\phi_{max}/\theta).$$

The output of the photodetector (in amps) for the case illustrated in Figure 4 is equal to **twice** the power in the shaded area (because the shaded area has been both subtracted from the lower half of the bi-cell and added to the upper half) times the radiant sensitivity of the photodetector, S (in amps/watt):

$$\text{output of the photodetector} = 2\,[1.273\,S\,P\,(\phi_{max}/\theta)].$$

Finally, the measured voltage, V_{max}, corresponding to a beam deflection of ϕ_{max}, is equal to the output of the photodetector times the input impedance, Ω (in ohms), of the measuring instrument (oscilloscope, lock-in amplifier, etc.):

$$V_{max} = 2\,[1.273\,\Omega\,S\,P\,(\phi_{max}/\theta)]. \qquad (5)$$

Equation (5) can be used for calibrating the PLD system once the physical parameters of the system are measured. A practical way of calibrating the system is to measure the bi-cell output for a known mass concentration of either soot or NO_2.

Parameter values typical of those applying to Phase I are presented in Table 1. Using these values, a 200 ppm NO_2 in N_2 gas mixture (i.e., 0.41 grams NO_2 per m^3) at 1 atmosphere pressure and 21°C is calculated, using Equation (3), to result in a probe beam deflection equal to:

$$\phi_{max} \simeq 1.2 \times 10^{-4} \text{ radians.}$$

Note, however, that a different expression and sensitivity would be predicted in the near field case where the probe laser is near the bi-cell detector and the laser beam remains essentially collimated.

TABLE 1. TYPICAL PARAMETER VALUES USED IN SENSITIVITY ANALYSIS

Parameter	Value
l	0.15 meters
n_o	1
$\partial n/\partial T$	9.2×10^{-7} K^{-1}
α	0.145 meters^{-1}
E_o	10 mJ/pulse
ρ_m	1.2 kg/m^3
c_p	1.014 kJ/kg-K
v_x	zero
a	0.001 meters

SECTION III

EXPERIMENTAL FACILITIES AND PROCEDURES

A. EXPERIMENTAL FACILITIES

The Phase I experimental facility is shown schematically in Figure 5. Two 4- by 8-foot optical tables were used to hold the lasers, optics, sample cell, photodetector, and soot generator.

The first optical table provided a stable platform for the pump laser combination: a Lumonics HyperEX-400 excimer laser and HyperDYE-300 tunable dye laser. The excimer laser was operated with XeCl in Neon at a repetition rate of 25 pulses per second. Each pulse had a duration of approximately 30 ns and contained approximately 200 mJ of energy at a wavelength of 308 nm. The output of the excimer laser was directed into the dye laser where it pumped a Coumarin 450 dye. The dye laser was tuned to provide a pulsed output at a wavelength of 451 nm, well into the region of NO_2 absorption (see Figure 6). The collimated dye beam (hereafter called the pump beam) traversed the 3 meters to the second optical table and was directed by two mirrors to the sample cell at an optical height of 12 cm. After emerging from the sample cell, the pump beam was directed to a calorimeter to measure beam power, which was typically between 2 and 7 mJ per pulse.

Note that the pump illumination source to be used both in a Phase II follow-on and in future prototypes is expected to be much simpler than the excimer/dye laser combination used in Phase I. As shown below, pulsed light sources (such as a Xenon lamp) provide sufficient energy per unit area to insure adequate probe beam deflection when measuring soot. These lamps cost approximately $1000 and may result in a very rugged and inexpensive field instrument.

The sample cell was a cylinder constructed of aluminum with a length of 30.5 cm and an inside diameter of 1.27 cm. Optical windows were attached to either end of the cell and were sealed with o-rings so that the cell was gas-tight. Fittings for 1/4-inch tubing were attached to the cell approximately 1 cm in from either end so that the soot or NO_2 samples traversed the length of the cell during analysis. The sample cell was wrapped with heating tape and kept slightly above the 31°C dew point of the effluent from the soot generator (described in Section IIIB, below) to preclude condensation of the effluent on the optical windows while measurements were taken. The sample cell was positioned so that the pump beam traversed the centerline of the cell.

The probe laser was a 5-milliwatt Spectra-Physics Model 147P Helium-Neon (HeNe) laser, operating at a wavelength of 633 nm. Beam diameter and divergence were 0.922 mm and 0.87 milliradians, respectively. The HeNe laser was placed close to the sample cell to minimize the diameter of the probe beam as it traversed the sample cell. The probe beam was steered to the cell by mirrors and traversed the cell at an angle of 0.75 degrees relative to the pump beam. This kept the pump and probe beams from overlapping on the windows to avoid the interaction of the probe beam with potential refractive index gradients in the windows created as a result of pump beam energy absorption by soot adhering to the windows during analysis. The crossing angle of 0.75 degrees resulted in an interaction length (i.e., the length of pump/probe beam overlap) of approximately 15 cm. Upon emerging from the sample cell, the probe beam was picked up by a prism and directed to a photodetector. (The prism insured that no pump beam energy was simultaneously directed to the photodetector.) The photodetector was a quadrant silicon photodiode (Silicon Detector Corporation Model SD 380-23-31-251) with a radiant

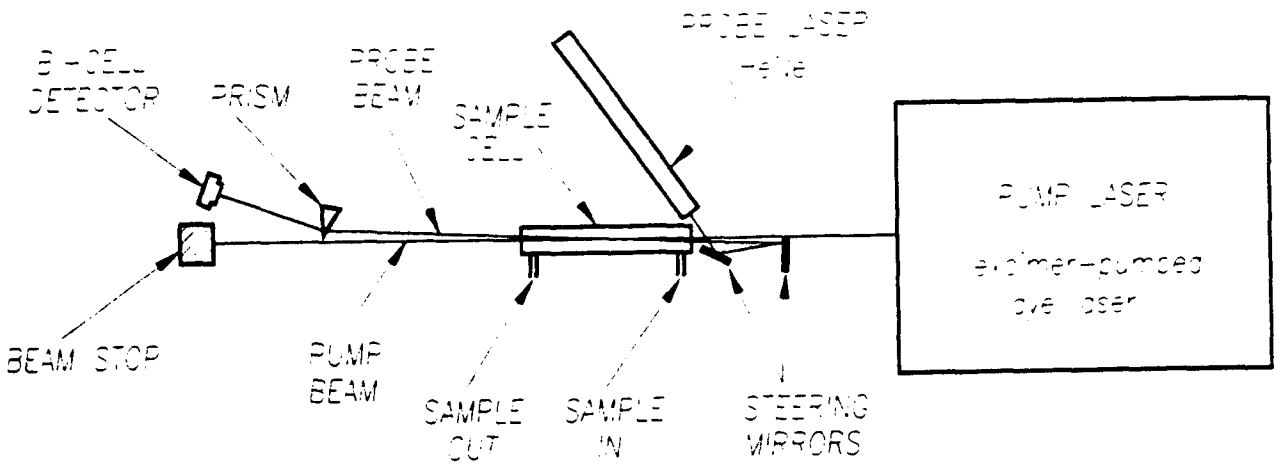

Figure 5. Schematic of Experimental Facility (Top View).

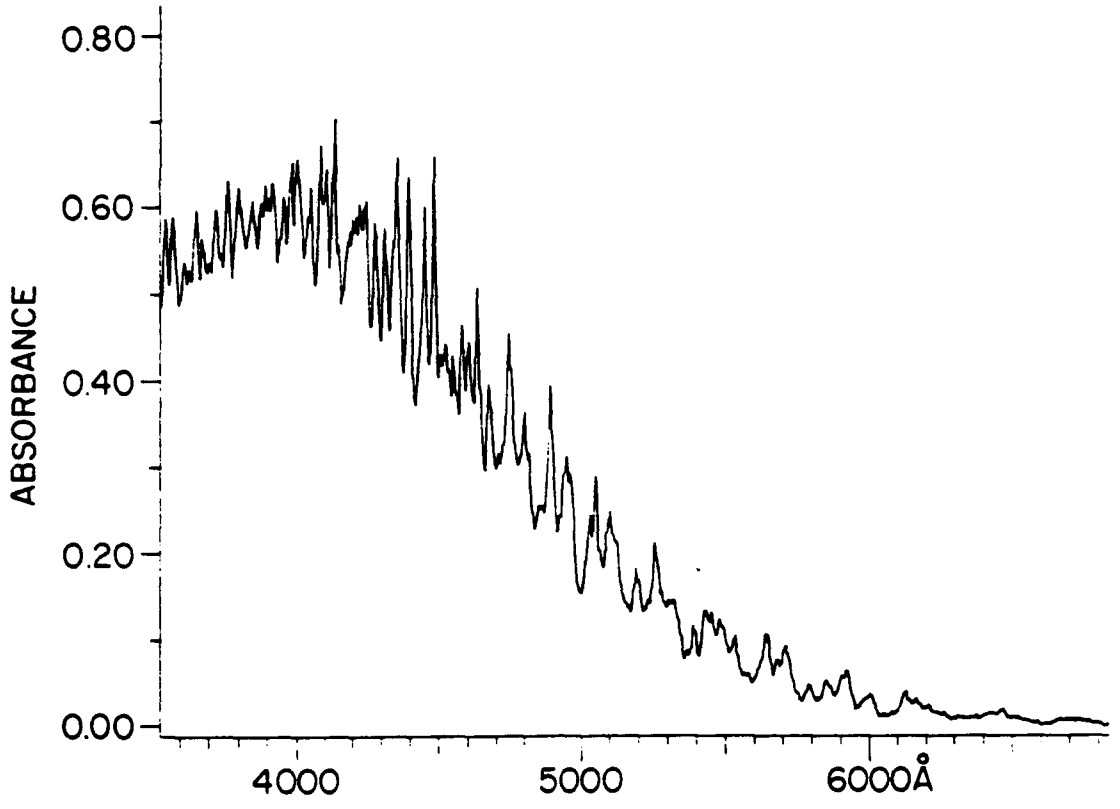

Figure 6. NO_2 Absorption Curve from 360 to 680 nm (Reference 19).

sensitivity of 0.35 amps/watts wired in a bi-cell configuration to sense probe beam motion normal to the optical table (i.e., in the vertical direction). The photodetector was housed in an aluminum enclosure fitted with an interference filter (Melles Griot catalog No. 03 FIL 006) with 46 percent transmission at 632.8 nm. Since neither the sample cell windows nor the prism were antireflection coated, the total beam power reaching the photodetector was approximately 1.8 milliwatts. The photodetector assembly was mounted on a traverse which provided precise alignment in the x-y plane. The total length of probe beam travel from the sample cell window to the photodetector was 75 cm.

The output of the photodetector was monitored with a Tektronix Model 5103N oscilloscope. It was amplified with a differential amplifier constructed at Vanderbilt University, and measured with an Ithaco Model 3941 lock-in amplifier with a time constant set at 30 seconds for the NO_2 measurements and 10 seconds for the soot measurements. Lock-in amplifier signal filters for the NO_2 measurements were set at 10 Hz for the high pass and 10 kHz for the low pass. Signal filters for the soot measurements were set at 10 Hz for the high pass and 100 Hz for the low pass. The reference signal fed to the lock-in amplifier was derived from a reference voltage sync pulse from the excimer laser. This sync pulse had an amplitude of approximately 25 volts and a duration of 100 ns, and preceded the emission of excimer light by approximately 100 ns. The excimer sync pulse was conditioned by a pulse counter/generator constructed at Vanderbilt University to make it compatible with the TTL input requirements of the lock-in amplifier.

NO_2 samples of known concentrations from 208 to 3.25 ppm in N_2 were produced by sequential dilution of a Matheson Gas Products 208 ppm NO_2 standard mixture. The dilution scheme is described below in Section IIIC.

Soot samples of known concentrations from 10 to 0.3 mg/m^3 were produced from the aerosol nebulizer described below. The nebulizer was connected to the "sample in" port of the sample cell (see Figure 5) with 1/4-inch diameter copper tubing. The distance from the exit of the soot generator to the sample cell was kept to approximately 15 cm and sharp bends in the tubing were avoided to minimize adsorption of the soot on the inside walls of the tubing.

B. AEROSOL SOOT GENERATOR

An aerosol nebulizer was used in Phase I to simulate jet engine and rocket exhaust by producing a synthetic soot/gas mixture of known carbon mass loading. The nebulizer produced a constant and known output of carbon particles at concentrations varying from 0.1 to 10 mg of carbon per m^3 of nitrogen. The principles of operation of the nebulizer and the procedure used to prepare the carbon/water nebulizer solutions are detailed here.

A commercial dispersion of carbon black (Penn Color product No. 31B107) provided the source of carbon used in the nebulizer. Its composition, in percent by weight, was as follows:

- 40.0 percent carbon black
- 46.5 percent water
- 6.5 percent acrylic resin (dispersing agent)
- 2.0 percent aqueous ammonia (for pH balance)
- 5.0 percent propylene glycol

Dilute solutions were made from the commercial dispersion for use in the nebulizer by adding a weighed quantity into a measured volume of water and agitating the mixture in a blender for several minutes. The initial dilution made in this manner was prepared by

adding 0.71 grams of commercial dispersion into a liter of distilled water. When nebulized under nominal conditions (described below), this solution produced a nebulizer output of 10 mg of carbon per m^3 of nitrogen. Less concentrated carbon aerosols (down to 0.1 mg carbon per m^3 of nitrogen) were produced by further dilution of the initial nebulizer solution.

The nebulizer (Inspiron Model 002305) was an aspirator/impingement type designed to operate at one atmosphere pressure. During operation, nitrogen was fed through a small orifice in the nebulizer cap where it was directed tangentially at high velocity over a hole through which a carbon/water mixture was aspirated from the nebulizer reservoir (shown schematically in Figure 7). This aspirated mixture was then blown against a small cylindrical protrusion inside the cap where the impact atomized the mixture into droplets with diameters between 2 and 5 micrometers.

The nebulizer was operated at a nitrogen flowrate of 8.5 liters per minute, where approximately 0.3 ml of the carbon/water mixture were atomized per minute. The nebulizer reservoir had a capacity of 0.5 liters of fluid, giving it many hours of uninterrupted operation. The soot (i.e., carbon) generation rate was controlled by choosing an appropriate carbon concentration in the water filling the nebulizer reservoir. For example, at a nitrogen flowrate of 8.5 liters per minute (the nominal flow condition), a carbon concentration of 2.8×10^{-4} grams of carbon per milliliter of water (which corresponded to 0.71 grams of the commercial dispersion per liter of water, described above) resulted in 10 mg of carbon per m^3 of nitrogen in the nebulizer aerosol. Simply diluting this solution by 10 times with water resulted in 1/10th the carbon concentration in the aerosol (i.e., 1.0 mg carbon per m^3 of nitrogen).

The carbon-laden droplets emerging from the nebulizer were then directed into a dryer consisting of a heated aluminum cylinder 3 inches in diameter and 24 inches in length (Figure 8). The dryer was wrapped with heating tape. In traversing the dryer, the carbon-laden droplets were evaporated, leaving the dried carbon suspended in the nitrogen.

After evaporation, the gas/particle mixture had a dew point above room temperature. The dew point is defined as the temperature at which a gas is saturated with water; it is a temperature below which the spontaneous condensation of water will occur. The dew point was determined from the humidity ratio, w, defined as the ratio of the mass of water vapor present, m_v, to the mass of dry air present, m_a, per unit volume:

$$w = m_v/m_a$$

For the conditions used in Phase I (a constant nitrogen flowrate of 8.5 liters per minute generating 0.3 cc of water aerosol per minute), the humidity ratio was:

$$w = (0.3 \text{ grams } H_2O)/(10.2 \text{ grams } N_2) = 0.029$$

This corresponded to a dew point of 31°C, as read from a psychrometric chart (Reference 18). As a result, the sample cell was heated slightly above this temperature with heating tape to preclude condensation on the optical windows while measurements were taken.

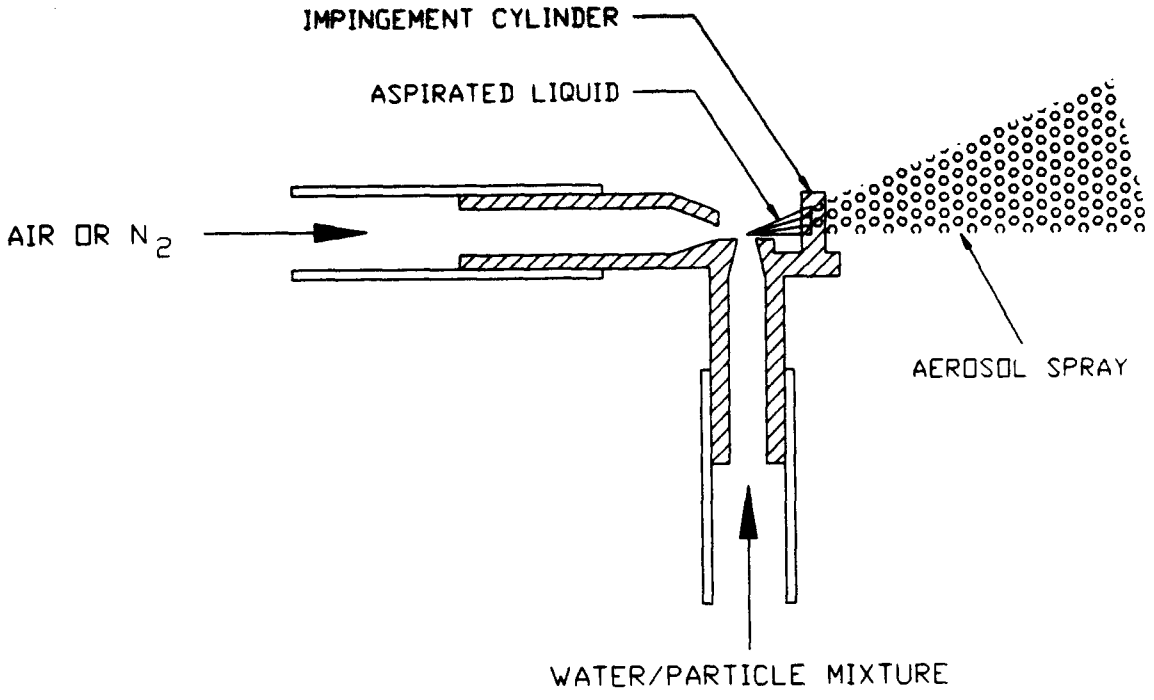

Figure 7. Schematic of Aerosol Nebulizer.

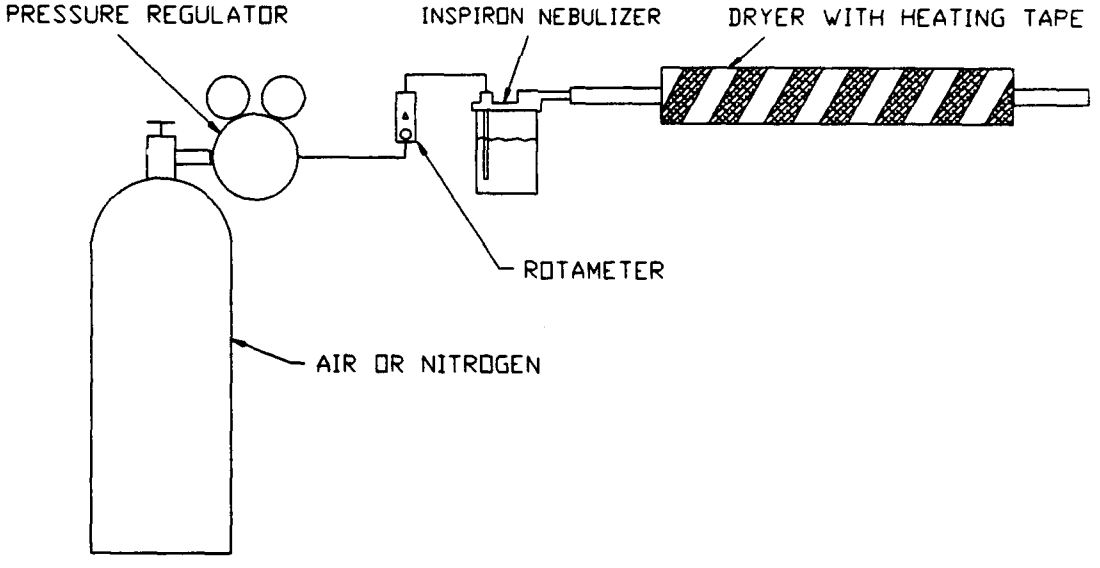

Figure 8. Schematic of Soot Nebulizer System with Dryer.

Figures 9 and 10 present transmission electron micrographs (TEMs) of carbon particles produced as described above. Taken at a magnification of 10,000 times, they are reproduced here at a scale of 1 micrometer per centimeter. Figure 9 presents particulate collected at the exit of the dryer at a concentration of 10 mg carbon per m^3, while Figure 10 presents particulate collected at a concentration of 0.1 mg carbon per m^3. The range of sizes is greater for the more concentrated case (Figure 9), where sizes range from approximately 0.1 to 2 micrometers, compared to the less concentrated case, where the particles seldom exceed 0.3 micrometers. Thus, it is evident that the smallest particle size attainable with the commercial dispersion is approximately 0.1 to 0.2 micrometers, and that these agglomerate to produce larger particles as final concentrations approach 10 mg carbon per m^3.

Figure 11 presents a TEM of a single 0.25 micrometer particle, originally taken at a magnification of 250,000 times, produced with the nebulizer/dryer at a carbon concentration of 10 mg/m^3. The TEM is reproduced at a scale of 0.04 micrometers per centimeter, and shows the particle to be composed of an agglomeration of 0.05 micrometer carbon spheres. With further processing of the carbon dispersion (i.e., with the further application of sufficient mechanical shearing in the presence of adequate dispersing agent), the agglomerates in the dispersion can be broken down to still smaller agglomerates until the 0.05 micrometer primary spheres are finally separated. This was not necessary for Phase I, however, and the commercial dispersion of carbon black was used as received by the manufacturer.

C. EXPERIMENTAL PROCEDURES

1. Nitrogen Dioxide Measurements

The proper operation of the PLD system was established by analyzing the series of NO_2 concentrations shown in Table 2. These values were chosen to cover the range of concentrations typically found in propulsion exhaust, and provided sufficient coverage to assess the relationship between NO_2 concentration and PLD signal intensity. These concentrations were produced by the sequential nitrogen dilution of a commercial 208 ppm NO_2 gas mixture as follows:

a. The sample cell was evacuated with a mechanical vacuum pump.

b. The sample cell was then filled to a pressure of 30 inches of mercury with the commercial 208 ppm NO_2 gas mixture, and PLD measurements were taken under static (no flow) conditions.

c. The sample cell was then partially evacuated to a pressure of 15 inches of mercury , and was filled back to 30 inches of mercury with high purity nitrogen, thus creating a 104 ppm NO_2 gas mixture. PLD measurements were then taken.

d. Step c. was repeated sequentially until measurements had been taken down to 3.25 ppm NO_2.

2. Soot Measurements

Soot measurements were made at the airborne carbon concentrations listed in Table 2. As with NO_2, the soot concentrations were chosen to cover the range typically found in propulsion exhaust, and provided sufficient coverage to assess the relationship between soot concentration and PLD signal insert intensity. These concentrations were produced by making stepwise dilutions of an aqueous solution initially containing 2.8×10^{-4}

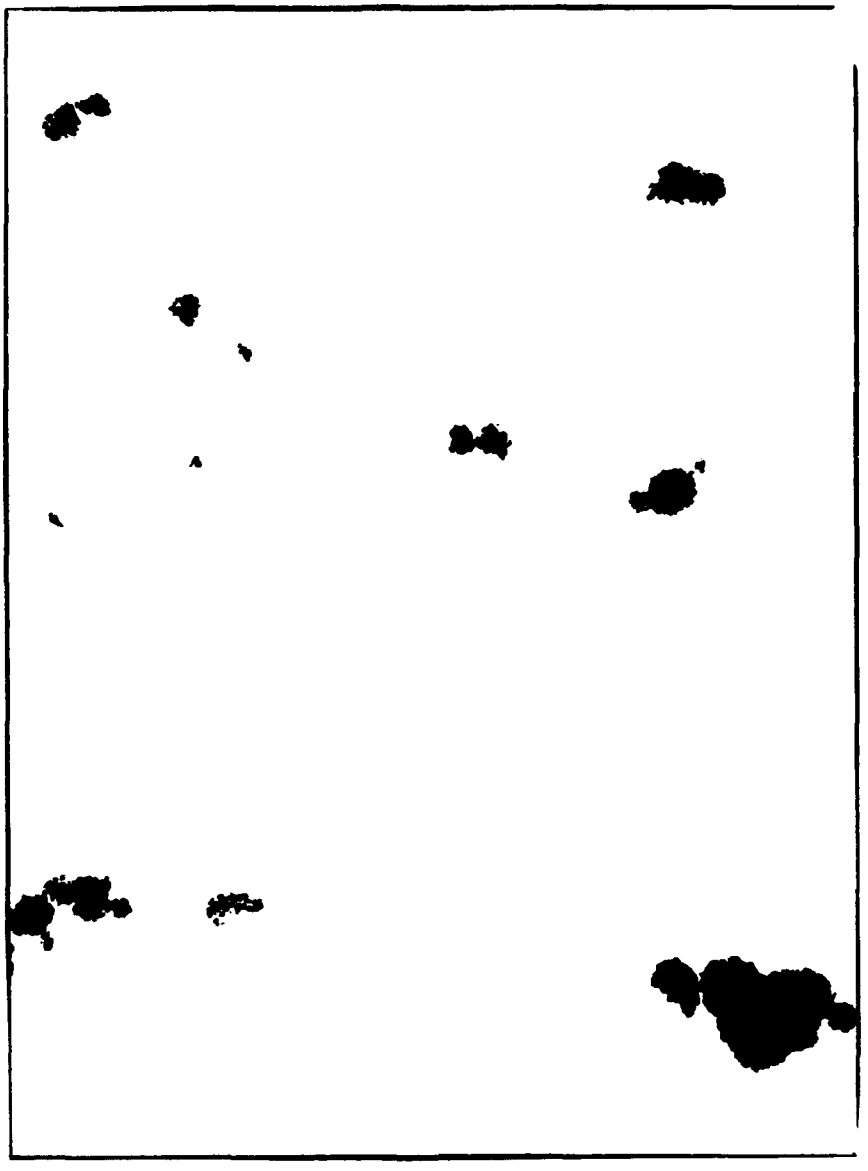

Figure 9. TEM of Carbon Particle Produced in Aerosol Nebulizer/Dryer at a Carbon Concentration of 10/mg/m^3, Reproduced at a Magnification of 10,000 Times.

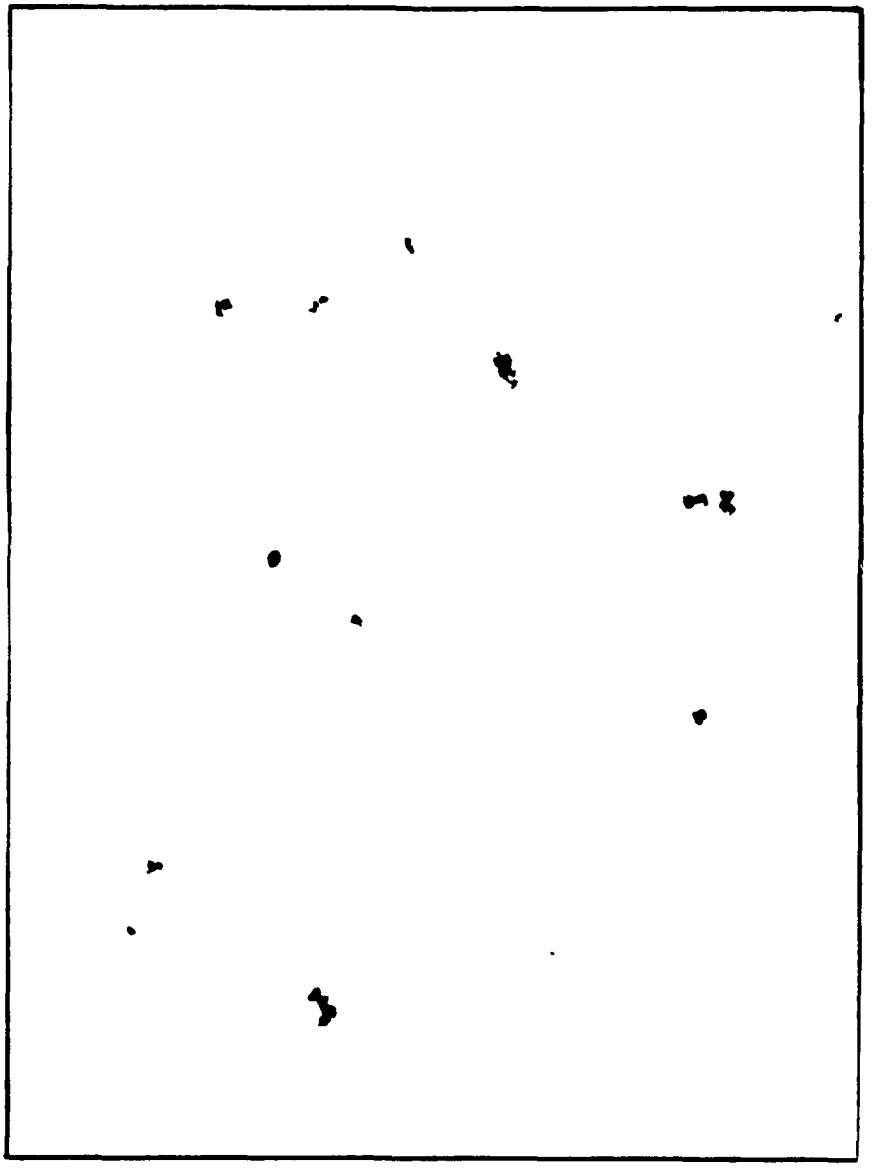

Figure 10. TEM of Carbon Particle Produced in Aerosol Nebulizer/Dryer at a Carbon Concentration of 0.1 mg/m^3, Reproduced at a Magnification of 10,000 Times.

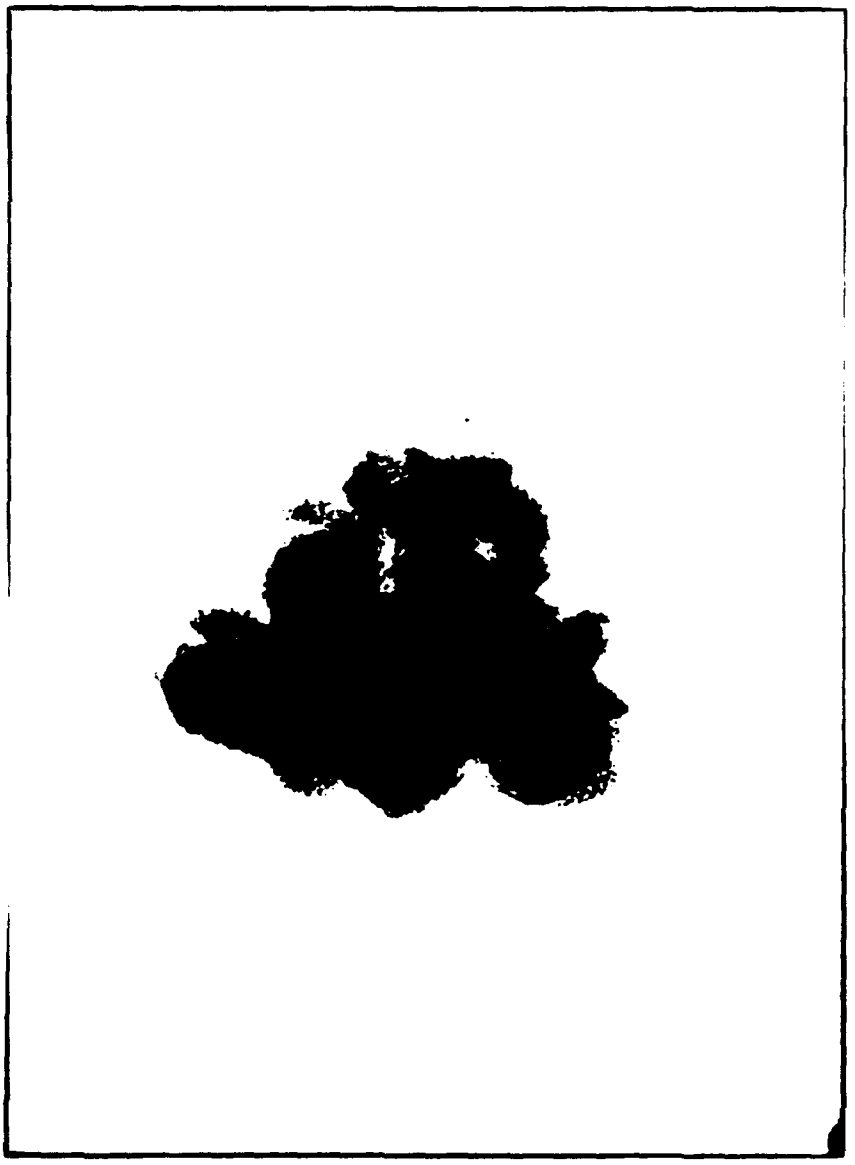

Figure 11. TEM of Single 0.25-Micrometer Particle Produced in Aerosol Nebulizer/Dryer at a Carbon Concentration of 10 mg/m^3, Reproduced at a Magnification of 250,000 Times.

grams of carbon per milliliter of water (see the procedure detailed in Section IIIB, above). The nebulizer was operated at a constant nitrogen flow rate of 8.5 liters per minute.

Prior to taking measurements, the soot nebulizer was operated for approximately 10 minutes to insure the sample cell contained a representative soot sample. The soot generator nitrogen flow was then turned off to allow experimental measurements to be made under static (i.e., no flow) conditions. This minimized background noise from the thermal gradients created as the relatively hot soot/gas mixture entered the sample cell. When measurements at a specific soot concentration were completed, the aqueous solution of carbon was diluted with distilled water and the measurement sequence was repeated at the new, lower concentration.

TABLE 2. NO_2 AND SOOT CONCENTRATIONS AND SIGNAL INTENSITIES

NO_2		Soot	
Concentration (ppm)	Normalized Signal Intensity (mV/mJ/pulse)	Concentration (mg/m^3)	Normalized Signal Intensity (mV/mJ/pulse)
208	0.631	10	0.399
104	0.315	3	0.145
52	0.161	0.9	0.035
26	0.083	0.27	0.006
13	0.041	0.1	----
6.5	0.030		
3.25	0.003		

SECTION IV

EXPERIMENTAL RESULTS AND DISCUSSION

A. NITROGEN DIOXIDE RESULTS

Figure 12 presents a graph of NO_2 concentration (in ppm) versus PLD signal intensity (in mV/mJ/pulse). The individual PLD signal intensities are given in Table 2. All signal intensities have been normalized to a constant pump beam power by dividing the output of the lock-in amplifier (in mV) by the pump beam power (in mJ/pulse). Figure 12 shows that the relationship between NO_2 concentration and normalized signal intensity is linear at NO_2 concentrations of 13 ppm and above. The deviation from linearity at a concentration of 3.25 ppm is a result of the low signal-to-noise ratio experienced at this low concentration with the breadboard system built for Phase I, and is not thought to result from inherent nonlinearities in the PLD technique itself. Steps that will significantly improve the signal-to-noise ratio of the current system are discussed in Section VC below. The observed linearity above 3.25 ppm is consistent with the theoretical prediction of Equation (4).

Figure 13 presents a graph of pump beam power (in mJ/pulse), measured after the sample cell, versus the measured PLD signal intensity (in mV), for a 208 ppm NO_2 sample. This relationship is also linear as predicted by Equation (3) in Section IIB.

Figure 14 presents a photograph of an oscilloscope trace showing a representative PLD signal taken with the 208 ppm NO_2 gas mixture. The signal is seen to nearly instantaneously deflect downward every 40 ms (i.e., 25 times per second) as the pump laser fires, and to return slowly to its baseline position during the ensuing 10 ms. This is consistent with the theoretical results reported in Reference 17. Although it was not measured in Phase I, the time scale associated with the leading edge is very short and is expected to be on the order of the laser pulse width. The time scale associated with the trailing edge is dictated by the diffusion time of the gaseous medium.

B. SOOT RESULTS

Figure 15 presents a graph of soot concentration (in mg/m^3) versus PLD signal intensity (in mV/mJ/pulse), while Table 2 lists the value of each individual PLD signal intensity. As explained above, all signal intensities have been normalized to a constant pump beam power by dividing the output of the lock-in amplifier (in mV) by the average pulse energy (in mJ/pulse). Figure 15 shows that the relationship between soot concentration and signal intensity is linear as predicted by Equation (4) in Section IIB. Note, however, that the signal from the 0.1 mg/m^3 soot sample was not measurable against the background noise experienced with the breadboard system built for Phase I.

Figure 16 presents photographs of two oscilloscope traces showing representative PLD signals for the 10 mg/m^3 soot sample. The photographs in Figures 16a and b show the signals obtained using a 100 Hz low pass filter and a 10 kHz low pass filter, respectively, on the lock-in amplifier. (A 100 Hz low pass filter was used to obtain the soot data presented in Figure 15.) The 100 Hz filter setting was initially chosen to provide better noise filtering than would have been provided by the 10 kHz setting used for the NO_2 measurements, and was based upon work reported in Reference 13 indicating that the probe beam deflection when analyzing soot was significantly slower than when analyzing NO_2. However, subsequent Phase I soot measurements taken at a low pass filter setting of 10 kHz showed that the filter setting of 100 Hz was rolling off the sharp deflection of the probe beam, and

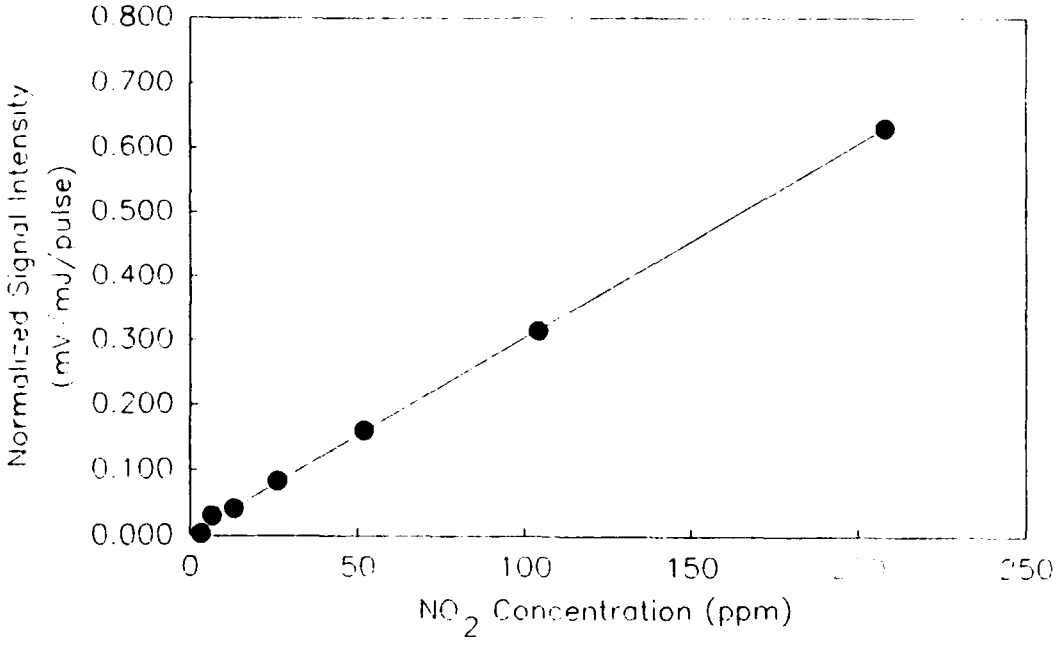

Figure 12. Graph of NO_2 Concentration (in ppm) Versus PLD Signal Intensity (in mV/mJ/Pulse).

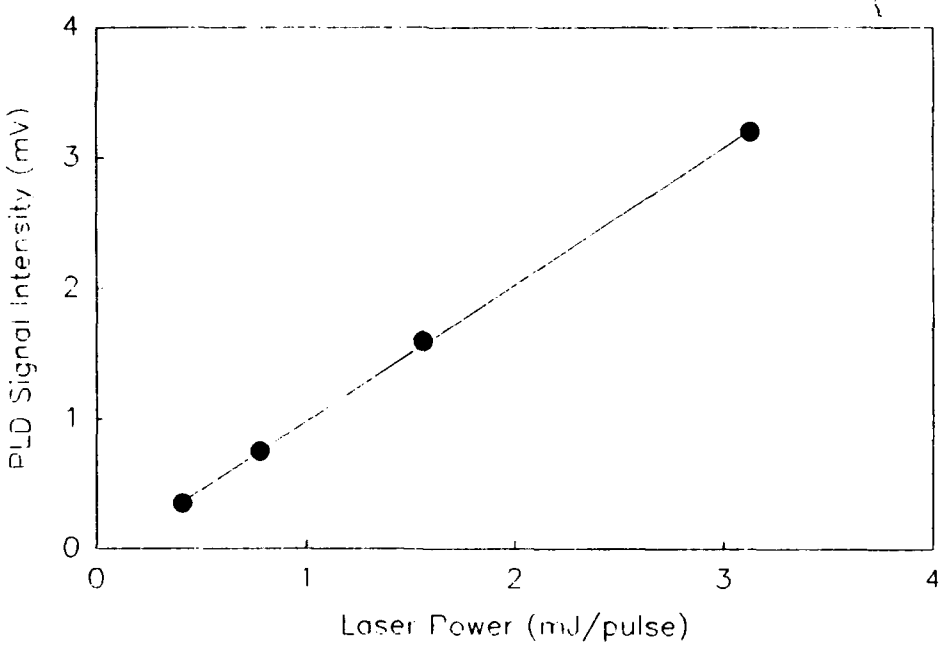

Figure 13. Graph of Pump Beam Power (in mJ/Pulse) Versus the Measured PLD Signal Intensity (in mV), for a 208 ppm NO_2 Sample.

Figure 14. Photograph of Oscilloscope Trace Showing a Representative PLD Signal Taken with the 208 ppm NO_2 Gas Mixture.

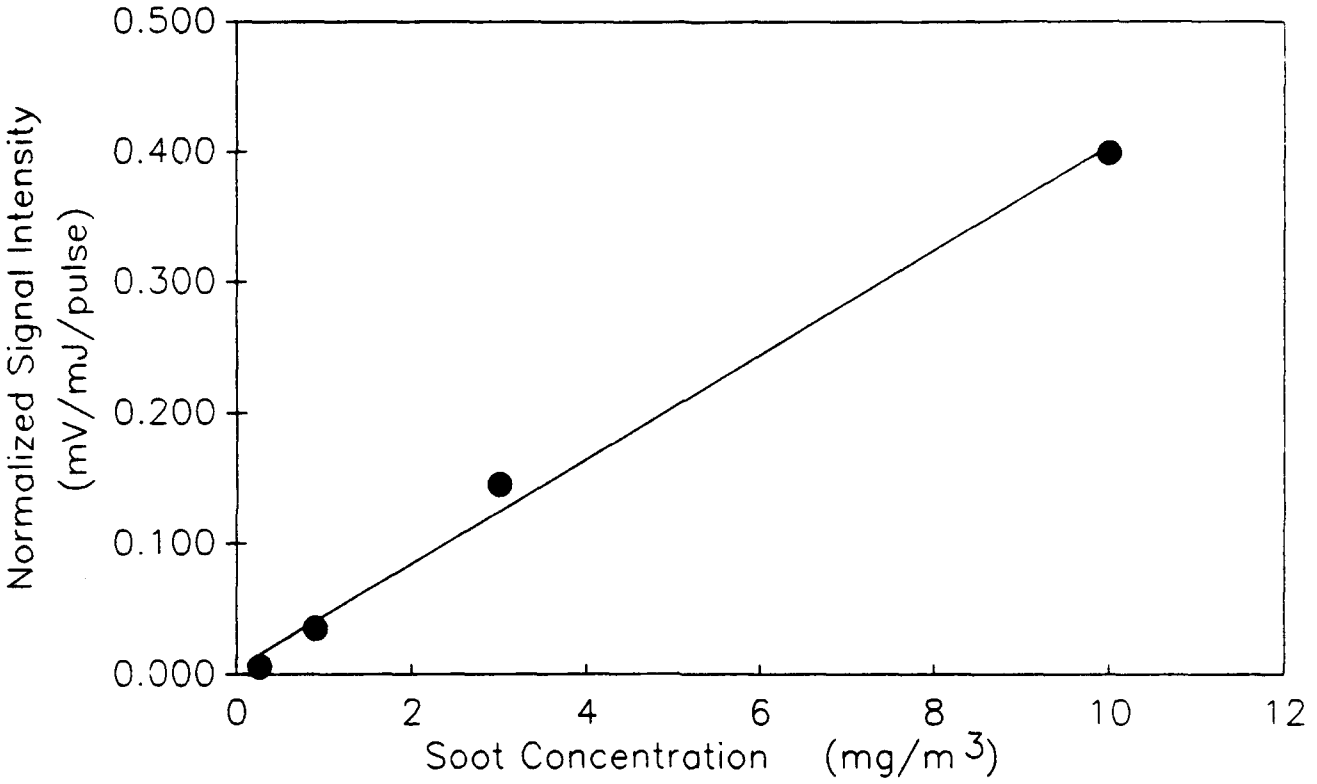

Figure 15. Graph of Soot Concentration (in mg/m^3) Versus PLD Signal Intensity (in mV/mJ/Pulse).

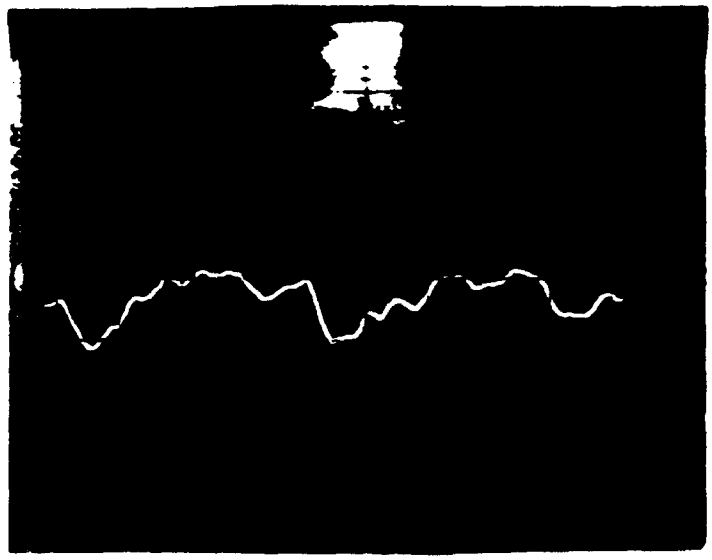

(a)

(b)

Figure 16. Photographs of Oscilloscope Traces Showing Representative PLD Signals for the 10 mg/m^3 Soot Sample using:

a. 100 Hz Low Pass Filter on the Lock-In Amplifier.
b. 10 kHz Low Pass Filter on the Lock-In Amplifier.

revealed that the true deflection when measuring soot occurred nearly as quickly as when measuring NO_2. This is evident when comparing Figures 14 and 16b. Although the amplitude of the soot signal is approximately 20 times less than the NO_2 signal, both the rapid deflection and the similarity in signal shape are evident.

a. 100 Hz low pass filter on the lock-in amplifier.
b. 10 kHz low pass filter on the lock-in amplifier.

The fast time scale associated with the rise of the leading edge of the soot signal suggests that it may be possible to measure soot in a turbulent flow using a lock-in amplifier or other frequency discriminator. Additional work must be performed during Phase II to evaluate the rise time of both soot-laden and gaseous media.

C. GENERAL DISCUSSION

While the experimental results presented above show linearity down to 0.3 mg/m^3 of soot and approximately 6 ppm of NO_2, these results by no means represent the lower limits of the technique. Significant improvements in sensitivity can be achieved by a combination of the following:

1. With a suitable choice of optics placed before the sample cell, the probe beam can be focused onto the face of the bi-cell detector, easily decreasing the beam spot diameter by a factor of four. All else being equal, a decrease in beam spot diameter will increase the bi-cell output by the same amount since a larger portion of the beam moves from one half of the bi-cell to the other for a given deflection. Since this reduced spot size increases the overall sensitivity of the bi-cell, it makes it also more susceptible to vibration and thermal fluctuations in the environment. Some of these noise sources can be minimized with a well-engineered system.

2. The probe beam power can be increased. This will increase the signal-to-noise ratio if the noise has an electrical origin or if the signal is photon-limited.

3. Measurement instrumentation and interconnection equipment must be carefully chosen to minimize electrical noise. To the extent that the overall background noise has an electrical origin, this will allow signals from smaller probe beam deflections to be discriminated from this background.

4. The interaction length, l, between the pump and probe beams can be increased. This is equivalent to decreasing the intersection angle between the two beams. The intersection angle of 0.75 degrees between the pump and probe beams in Phase I could not be decreased further because of the geometry of the mirrors used to steer the HeNe probe beam into the sample cell. Therefore, the interaction length of 15 cm could not be increased. However, the use of a dichroic mirror made to transmit the pump beam while reflecting the probe beam would eliminate the conventional mirrors and mounts used in Phase I and would allow intersection angles smaller than 0.75 degrees. (Note that the intersection angle must not be so small as to allow the pump and probe beams to overlap on the windows, as explained in Section IIIA.)

5. The **pump beam** path length from the laser to the sample cell can be shortened considerably compared to that used in Phase I. (The long path length of approximately 5 meters used in Phase I was dictated by the size of the specific lasers used in this work and by laboratory space constraints). A shorter path length will decrease the unwanted deflection of the pump beam by ambient thermal gradients present between the pump laser and the sample cell, which will decrease the wandering of the pump beam

within the sample cell. This will result in greater spatial stability of the thermal gradient established within the sample cell when the sample absorbs energy from the pump beam, which will stabilize the deflection of the **probe beam** as it interacts with this induced thermal gradient.

6. The **probe beam** path length from the laser to the sample cell should be minimized and the path should be insulated to decrease the detrimental interaction between the probe beam and any ambient thermal gradients outside the sample cell. This will decrease the unwanted, erratic movements of the probe beam on the face of the detector caused by ambient thermal gradients, which will decrease background noise and increase the signal-to-noise ratio.

7. The **probe beam** path from the sample cell to the detector should be insulated from ambient thermal gradients, whose effect on the probe beam is described above, and the path length should be optimized. Note that there is a trade-off in shortening the distance from the sample cell to the detector: a shorter distance decreases the interaction between the probe beam and ambient thermal gradients (which decreases background noise), yet decreases the movement of the probe beam on the face of the detector (which decreases the output of the detector). Further work is necessary to determine the optimal distance between the sample cell and the detector.

At the other end of the concentration spectrum, the PLD technique is capable of measuring concentrations much higher than the 208 ppm of NO_2 and 10 mg/m^3 of soot analyzed in Phase I. Calculations show that the probe beam deflects on the face of the detector less than 10 percent of its diameter for the 200 ppm NO_2 case. (This result is based on a nominal beam deflection of 1.2×10^{-4} radians, calculated in Section IID using Equation 3, and a probe beam diameter of 1.4 mm at the detector face, which takes into account the natural divergence of the probe beam over the distance from the HeNe probe laser to the detector.) Thus, more concentrated samples of either NO_2 or soot should be measurable before the beam has been deflected completely into one-half of the bi-cell detector, at which point the output stops increasing altogether. It is instructive to note that the output of the detector will become increasingly nonlinear as the pollutant concentration increases because of the circular area of the beam on the detector face. This does not make PLD unusable at much higher concentrations; it is only necessary to calibrate the response of the instrument in this nonlinear region. The linearity of the data presented in Section V corroborates the conclusion above that the probe beam deflected only a fraction of its diameter at the highest concentrations measured in Phase I.

The application of the PLD technique is potentially far-ranging because of its fast time response. The nearly instantaneous results make it an excellent candidate for in-line, real-time measurements. Perhaps the most common application of PLD will be in a configuration where samples are extracted from a measurement medium such as the exhaust of a rocket, gas turbine engine, diesel engine, or industrial smokestack.

It is also probable that, under some conditions, PLD will provide *in situ* measurements in these environments. The success of *in situ* measurements will depend upon both the relative magnitude of the turbulence scale of the flow and the time scale of the PLD signal. Note that the PLD signal is the result of a density change imposed by the pump beam as it heats the medium. Turbulent flows, especially those in a combustion environment, have natural density fluctuations which will also cause the probe beam to be deflected. These flow fluctuations typically take place on a time scale on the order of 0.1 ms (i.e., with frequencies on the order of tens of kHz). The time scale of the PLD signal associated with **gaseous** measurements is on the order of tens of nanoseconds, so that it is approximately 10,000 times faster than the time scale of natural density fluctuations in

practical turbulent flows. Therefore, it is anticipated that a two-channel gated integrator will be capable of distinguishing the PLD signal from the background turbulence.

In the case of soot, however, *in situ* measurements may not always be possible in a hot, turbulent flow because of the slower time scale associated with the heat transfer from the soot to the surrounding gas when using a low energy pump source. However, a high-energy pump source may vaporize the soot particles, resulting in an almost instantaneous heat transfer to the surrounding gas (Reference 12). This was apparently the case in Phase I using a pump beam energy of approximately 5 mJ/pulse. While the rise time was not accurately measured, it was estimated to be on the same order as the rise time of the NO_2 measurements, providing evidence that the soot was vaporizing during pump beam exposure. Additional measurements will be required during Phase II to obtain the functional relationship between soot particle size and concentration, pump beam power density, and the PLD time scale.

SECTION V

PROTOTYPE CONCEPTS

The high cost and complexity of an excimer/dye laser combination is not required to make PLD measurements. In fact, static cell soot measurements can be performed with a simple pump light source such as an arc lamp or a diode laser. The work completed in Phase I has lead to the development of several PLD prototype concepts differing, in part, from the breadboard system used in Phase I in the source of pump light used to create the necessary thermal gradient within the sample. These concepts are being developed with the goal of producing a durable, versatile instrument of small size and weight, while keeping expected costs at a minimum. This section describes some of these prototype concepts. Other concepts will evolve during Phase II in an effort to match the requirements of the Air Force and industry.

1. Arc Lamp Concept

Equation (3) (Section IIB) indicates that the PLD signal is directly proportional to the laser energy, E_o, and to the pump/probe beam interaction length, l. It is also inversely proportional to a^3. Phase I experimental results were obtained with a pulsed excimer-pumped dye laser which delivered E_o = 3 to 7 mJ into a probe volume with a cross sectional area of a^2 = 2 mm^2 and a length of l = 15 cm. Thus, the PLD signal in Phase I was proportional to $E_o l/a^3$ = 250 mJ/mm^2 (assuming 5 mJ/pulse). Since soot absorbs light essentially as a black body at visible wavelengths, a white light source, such as an arc lamp, will match this energy requirement. Commercial arc lamps (e.g., ORC model AP 101) deliver from 200 J/s (Joules/second, or Watts) to 1500 J/s **continuously** into an equivalent volume of about 275 mm^3. Assuming 200 J/s into a volume 6.5 mm on a side, the parameter $E_o l/a^3$ will be equal to 250 mJ/mm^2 when the exposure time is approximately 50 ms. Thus, the continuous output from a 200 Watt arc lamp, chopped at 10 Hz with a 50 percent duty cycle (i.e., the sample would be illuminated for 50 ms out of every 100 ms) would result in the same pump energy being deposited into a sample as in Phase I, and would still allow sufficient time for the absorbed energy to diffuse away from the probe volume (which takes approximately 5 ms under static conditions).

The arc lamp appears to be ideally suited for soot measurements, and possibly gaseous pollutants with a broad absorption band such as NO_2, provided that other major constituents are not present at the same time. To use the arc lamp in the simultaneous measurement of soot and NO_2, the white light would be divided into two bands: one lower than 600 nm (where it is absorbed by NO_2 and soot), and the other higher than 600 nm (where it is only absorbed by soot). These two simultaneous measurements will provide the mass concentration of both species.

2. Laser Diode Concept

Commercial laser diodes can deliver up to about 1 Watt of continuous monochromatic radiation between wavelengths of 750 and 850 nm. The beam cross section of these lasers is very similar to the beam cross section of the dye laser used in Phase I. Therefore, if the energy per chopping interval is matched to the value of approximately 5 mJ/pulse used in Phase I, we can expect the diode laser to produce as much deflection as was obtained with the excimer-pumped dye laser. This energy requirement can be matched with a 5 ms or longer illumination time, which is equivalent to a chopping frequency of 100 Hz or less (this assumes a 50 percent duty cycle). Larger amounts of energy would be available at slower chopping rates.

Laser diodes are tunable over a narrow wavelength range. Thus, it is conceivable that the diode laser could be tuned to be transparent to all the gaseous species present in a sample, such that only soot would absorb the pump radiation.

One drawback of the laser diode is that there are no currently available models with wavelengths below approximately 680 nm, so that NO_2, for example, is beyond the reach of a PLD instrument employing such a laser.

SECTION VI

CONCLUSIONS AND RECOMMENDATIONS

A. CONCLUSIONS

The experiments and analyses conducted during Phase I have demonstrated the feasibility of PLD in measuring the mass concentration of both soot particles and the gaseous pollutant NO_2 over broad dynamic ranges of interest to the gas turbine and rocket communities. The specific accomplishments of the current program include:

1. The design, construction, and successful operation of a breadboard PLD system constructed specifically for this Phase I program utilizing an excimer-pumped dye laser as a pump source and a Helium-Neon laser as the probe.

2. The demonstration of a linear response when measuring NO_2 at concentrations from approximately 6 to 200 ppm.

3. The demonstration of a linear response when measuring soot at concentrations from 0.3 to 10 mg/m^3.

4. The demonstration of PLD measurements at a repetition rate of 25 Hz.

5. The design, construction, and successful operation of a soot generator utilizing an aerosol nebulizer. This soot generator allowed the quantitative production of carbon particles spanning soot concentrations from 0.1 to 10 mg/m^3.

Thus, the PLD technique has been shown to be more sensitive and faster than other commonly used methods, and measures the concentration of gaseous pollutants such as NO_2 which are not possible with techniques involving filtering. Furthermore, its fast time response makes it an excellent candidate for *in situ* measurements under many conditions.

B. RECOMMENDATIONS

The completion of the Phase I technical effort has resulted in the following recommendations:

1. A survey should be taken of industry and government to precisely determine customer needs and to understand the range of potential applications that may be addressed by the PLD technique. This survey will define the type and range of the most important polluting particles, and the most important gaseous pollutants, including the spectral lines which may be pumped. This will allow the development of a versatile instrument with features that are attractive to potential users.

2. The relative time scale associated with the leading edge of the PLD signal should be evaluated for both soot and gaseous species. An understanding of this phenomenon will influence the choice of instrumentation and signal processing used to optimize measurement speed and accuracy, and will answer questions regarding the application of PLD to turbulent and/or combusting flows. Additional work must also be performed to elucidate any functional relationship between PLD time scale and particle size to insure the accurate interpretation of measurement results.

3. The relative contribution of electrical and optomechanical noise to the overall noise background must be investigated further. This will allow the sensitivity of the PLD technique to be maximized in the most effective way.

4. The actual measurement of the PLD signal deserves further investigation. Questions remain as to whether the peak value of the PLD signal or the integrated area of the signal provides a more effective measure of the concentration of the absorbing species. Although either parameter may provide accurate concentration data, measuring one or the other may require less expensive equipment and/or less complex data processing algorithms.

5. The optimum separation distance between the sample cell and the detector must be determined to minimize background noise from ambient thermal gradients while providing the maximum deflection of the probe beam on the face of the detector (thus maximizing sensitivity).

6. The anticipated nonlinear detector response at high species concentration must be investigated. (Note that the concentrations of soot and NO_2 were not high enough in Phase I to show this nonlinearity.) An understanding of this phenomenon should allow the application of the PLD technique to concentrations much higher than those used in Phase I.

7. An analytical model should be developed relating solid particulate (i.e., soot or asbestos) concentration to PLD signal shape and intensity. The insight this would provide is essential to the development of an effective and versatile instrument.

8. It should be determined whether, or to what extent, the absorption coefficient of soot is dependent on combustor geometry and operating conditions, fuel composition, particle size distribution, volatile content, etc. The absorption coefficient is a very important parameter in PLD. Accurate values are often difficult to determine in many cases, and uncertainties or inaccuracies in its value result in corresponding errors in the determination of species concentration.

9. An alternative must be found to the excimer/dye laser combination used in Phase I. There are several promising candidates (i.e., arc lamps or diode lasers), but a choice must be made based on the evaluation of many factors such as pulsed versus continuous output, wavelength, tunability, beam power, size, and ruggedness.

The above nine recommendations are not meant to be exhaustive. These and other recommendations will be discussed in detail in the Phase II proposal.

REFERENCES

1. Boccara, A.C., D. Fournier, W.B. Jackson, and N.M. Amer, "Sensitive Photothermal Deflection Technique for Measuring Absorption in Optically Thin Media," Optical Letters, Vol. 5, p. 377, 1980.

2. Fournier, D., A.C. Boccara, N.M. Amer, and R. Gerlach, "Sensitive in situ Trace-Gas Detection by Photothermal Deflection Spectroscopy," Applied Physics Letters, Vol. 37, p. 519, 1980.

3. Jackson, W.B., N.M. Amer, A.C. Boccara, and D. Fournier, "Photothermal Deflection Spectroscopy and Detection," Applied Optics, Vol. 20, p. 1333, 1981.

4. Loulergue, J.C., and A.C. Tam, "Noncontact Photothermal Probe Beam Deflection Measurement of Thermal Diffusivity in a Hot Unconfined Gas," Applied Physics Letters, Vol. 46, p. 457, 1985.

5. Sell, J.A., "Gas Velocity Measurements Using Photothermal Deflection Spectroscopy," Applied Optics, Vol. 24, p. 3725, 1985.

6. Sontag, H., and A.C. Tam, "Time-Resolved Flow-Velocity and Concentration Measurements Using a Traveling Thermal Lens," Optical Letters, Vol. 10, p. 436, 1985.

7. Tam, A.C., H. Sontag, and P. Hess, "Photothermal Probe Beam Deflection Monitoring of Photochemical Particulate Production," Chemical Physics Letters, Vol. 120, p. 280, 1985.

8. Kizirnis, S.W., R.J. Brecha, B.N. Ganguly. L.P. Goss, and R. Gupta, "Hydroxyl (OH) Distributions and Temperature Profiles on a Premixed Propane Flame Obtained by Laser Deflection Techniques," Applied Optics, Vol. 23 p. 3873, 1984.

9. Rose A., J.D. Pyrum, C. Muzny, G.J. Salamo, and R. Gupta, "Application of the Photothermal Deflection Technique to Combustion Diagnostics," Applied Optics, Vol. 21, p. 2663, 1982.

10. Rose A., J.D. Pyrum, G.J. Salamo, and R. Gupta, "Photoacoustic Spectroscopy and Photothermal Deflection Spectroscopy: New Tools for Combustion Diagnostics," in Proceedings, International Conference on Lasers '82, R.C. Powell, Ed., STS Press, McLean, VA. 1983.

11. Rose A. and R. Gupta, "Combustion Diagnostics by Photodeflection Spectroscopy," in Twentieth Symposium (International) on Combustion, The Combustion Institute, Pittsburgh, PA, 1984.

12. Rose A. and R. Gupta, "Application of Photothermal and Photoacoustic Deflection Techniques to Sooting Flames: Velocity, Temperature, and Concentration Measurements," Optical Communications, Vol. 56, p. 303, 1986.

13. Pitz, R.W., "Advanced Optical Smoke Meters for Engine Exhaust Measurement," NASA Lewis Report Number NASA CR-179459.

14. Sell, J.A., Ed., Photothermal Investigations of Solids and Fluids, Academic Press, San Diego, CA, 1989.

15. Tam, A.C., "Applications of Photoacoustic Sensing Techniques," Reviews of Modern Physics, Vol. 58, p. 381, 1986.

16. Bialkowski, S.E., "Pulsed-Laser Photothermal Spectroscopy," Spectroscopy, Vol. 1, Number 10, 1986.

17. Rose A., R. Vyas, and R. Gupta, "Pulsed Photothermal Deflection Spectroscopy in a Flowing Medium: a Quantitative Investigation," Applied Optics, Vol. 25, p. 4626, 1986

18. Wark, K., Thermodynamics, McGraw-Hill Book Co., pg. 814, 1983.

19. Hsu, D.K., Monts, D.L., and Zare, R.N., Spectral Atlas of NO_2- 5530 to 6480 Å, p. 6, Academic Press, New York, 1978.